




Review

Carbon Nanostructures Decorated with Titania: Morphological Control and Applications

Maria Cristina Cringoli ^{1,2} , Siglinda Perathoner ^{3,4}, Paolo Fornasiero ^{1,2,5}  and Silvia Marchesan ^{1,2,*} 

¹ Chemical and Pharmaceutical Sciences Department, University of Trieste, 34127 Trieste, Italy; mcringoli@units.it (M.C.C.); pforasiero@units.it (P.F.)

² National Interuniversity Consortium of Materials Science and Technology (INSTM), University of Trieste, 34127 Trieste, Italy

³ Dipartimento di Scienze Chimiche, Biologiche, Farmaceutiche e Ambientali, University of Messina, 98168 Messina, Italy; siglinda.perathon@unime.it

⁴ National Interuniversity Consortium of Materials Science and Technology (INSTM), University of Messina, 98168 Messina, Italy

⁵ Istituto di Chimica dei Composti Organometallici, Consiglio Nazionale delle Ricerche (ICCOM-CNR), 34127 Trieste, Italy

* Correspondence: smarchesan@units.it; Tel.: +39-040-5583923

Abstract: Nanostructured titania (TiO₂) is the most widely applied semiconducting oxide for a variety of purposes, and it is found in many commercial products. The vast majority of uses rely on its photo-activity, which, upon light irradiation, results in excited states that can be used for diverse applications. These range from catalysis, especially for energy or environmental remediation, to medicine—in particular, to attain antimicrobial surfaces and coatings for titanium implants. Clearly, the properties of titania are enhanced when working at the nanoscale, thanks to the increasingly active surface area. Nanomorphology plays a key role in the determination of the materials' final properties. In particular, the nucleation and growth of nanosized titania onto carbon nanostructures as a support is a hot topic of investigation, as the nanocarbons not only provide structural stability but also display the ability of electronic communication with the titania, leading to enhanced photoelectronic properties of the final materials. In this concise review, we present the latest progress pertinent to the use of nanocarbons as templates to tailor nanostructured titania, and we briefly review the most promising applications and future trends of this field.

Keywords: titania; anatase; rutile; carbon; nanotubes; nanoparticles; nanorods; nanosheets; graphene; photocatalysis



Citation: Cringoli, M.C.; Perathoner, S.; Fornasiero, P.; Marchesan, S. Carbon Nanostructures Decorated with Titania: Morphological Control and Applications. *Appl. Sci.* **2021**, *11*, 6814. <https://doi.org/10.3390/app11156814>

Academic Editors: Petr Korusenko and Sergey Nesov

Received: 25 June 2021

Accepted: 23 July 2021

Published: 24 July 2021

Publisher's Note: MDPI stays neutral with regard to jurisdictional claims in published maps and institutional affiliations.



Copyright: © 2021 by the authors. Licensee MDPI, Basel, Switzerland. This article is an open access article distributed under the terms and conditions of the Creative Commons Attribution (CC BY) license (<https://creativecommons.org/licenses/by/4.0/>).

1. Introduction

1.1. Titania Properties and Uses

Titanium dioxide or titania is certainly the most studied semiconducting oxide due to its well-established photo-activity. Well-known features that render it so attractive are its low cost, negligible toxicity, high stability, easy handling, and resistance to chemical corrosion. This semiconductor has the known ability to absorb light in the ultraviolet (UV) wavelength range and generate excited charges, electrons and holes, which separate in the conduction and valence band, respectively, and are at the core of its photo-activity. This key property of TiO₂ has been widely investigated firstly in catalysis and later in medicine, especially to attain antimicrobial coatings for medical implants [1]. The wide applications of titania for air and water remediation, cultural heritage preservation, and self-healing, as well as microbial inactivation and the mitigation of SARS-CoV-2 spreading onto surfaces, have been recently reviewed [2] and are thus not discussed in detail in this review.

Despite the many advantages offered by titania, this material also suffers from some drawbacks, such as a rapid recombination of the photo-excited charge carriers and the relatively wide band gap (in the range of 3.2 eV) which implies a poor utilization of solar

light due to the small percentage of UV radiation of sunlight reaching the Earth's surface. Remedies that have been developed to address these issues include the use of suitable supports [3], doping with other elements [4], embedding in composites [5], and the development of suitable nanostructures [6], also following green protocols [7]. These approaches have indeed allowed the practical widespread use of TiO_2 —for instance, for biomass conversion processes [8]—thanks to the improved hydrothermal stability of the catalyst [9]. In particular, the combination of titania with noble metals and carbon nanostructures has allowed the development of high-performing gas sensors [10] and photocatalysts [11]. Dye-sensitizers combined with titania allow metal-free photocatalysts to be attained for hydrogen production using visible light [12]. Hydrogen-peroxide production is another area in which titania is highly promising [13], as well as solar cells [14].

The morphology and crystallinity of the titania phase are important parameters in the determination of the resulting photo-electronic properties of the final material [15]. However, only a few studies compare the photo-activity of the three phases of titania (rutile, brookite, and anatase; Figure 1) [16], while the majority of works focus on the generally best-performing anatase phase [17]. Titania can be produced by several methods, with sol-gel [18], hydrothermal [19], and solvothermal [20] processes being the most popular, and in some cases also microwave-assisted methods [21]. However, other approaches are also often used, such as anodic oxidation [22] and atomic layer deposition [23], and others are under continuous development; for instance, the use of laser beams [24], molecular layer deposition [25], and air-plasma spraying [26].

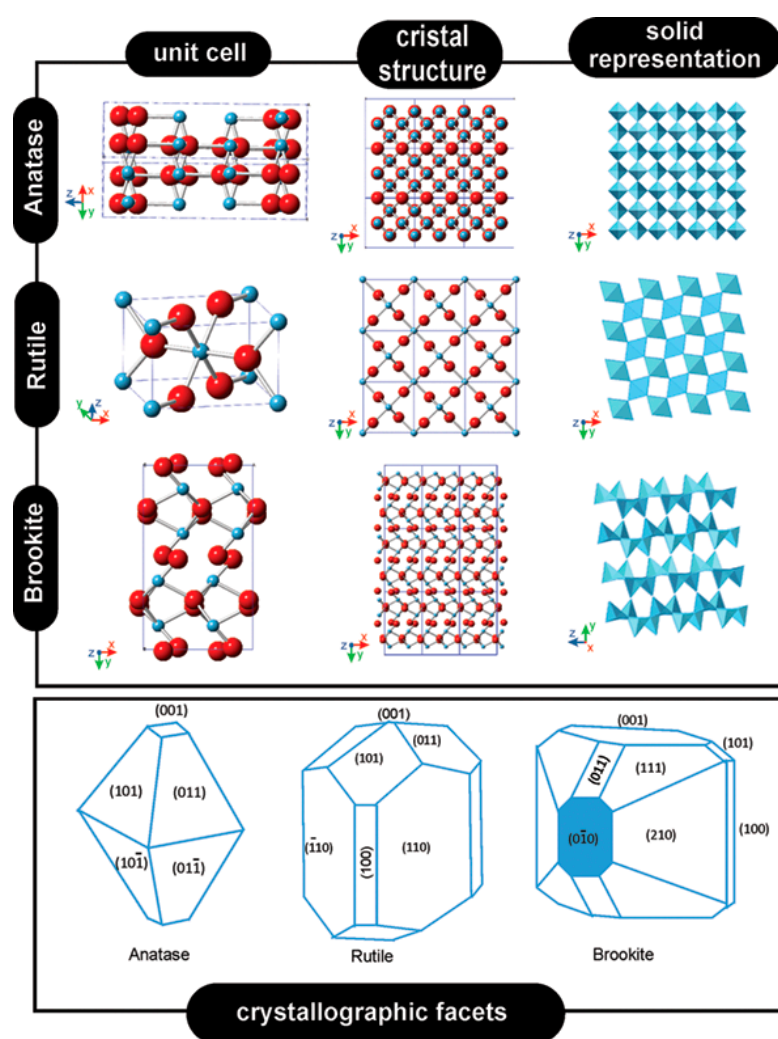


Figure 1. Crystal structures of titania anatase, rutile, and brookite polymorphs. Reprinted from [21].

1.2. Carbon Nanostructures Properties and Uses

Carbon nanostructures represent a large family of materials based on carbon characterized by a diversity of morphologies and structures (Figure 2) [27]. Typically, they present very interesting electronic and conductive properties that arise from the extended conjugation of sp^2 atoms, although exceptions exist. For instance, nanodiamonds contain mainly sp^3 -hybridized carbon atoms, as the name suggests [28]. Nanocarbons have been engineered to feature sp -hybridized carbon atoms as well, especially for energy conversion and storage applications [29]. In particular, sp -hybridized one-dimensional “synthetic carbon allotropes” are emerging as attractive molecular wires for advanced applications in electronics and opto-electronics [30].

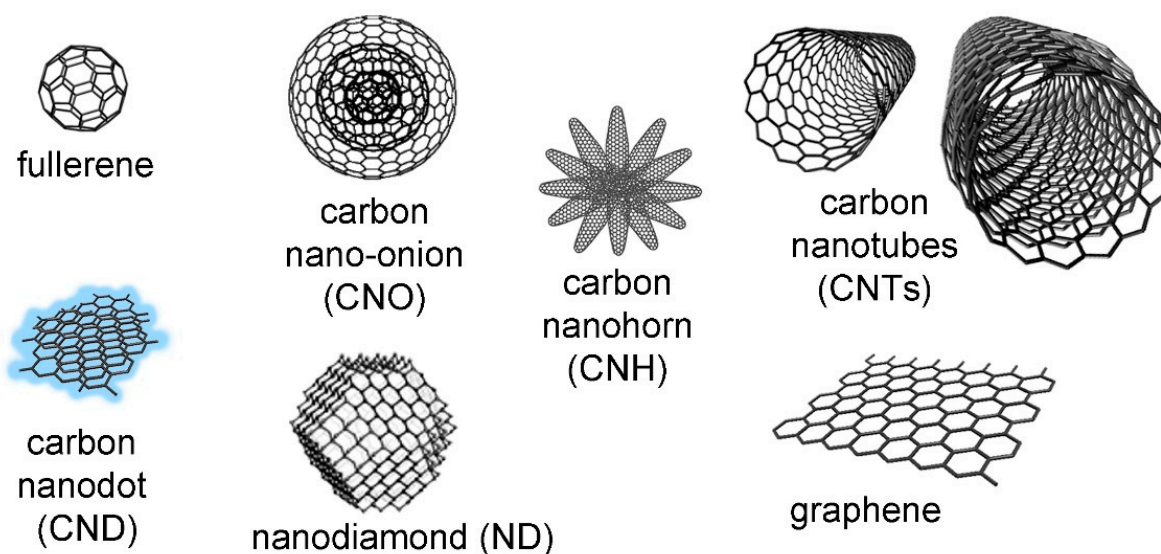


Figure 2. Different types of well-known carbon nanostructures (not to scale). Reproduced from [31]. The nano-onion is reproduced with permission from [32], copyright © 1996, Elsevier.

Among the most studied carbon nano-allotropes are zero-dimensional fullerenes [33], which can be considered as soccer-ball shaped structures, one-dimensional carbon nanotubes (CNTs), which have a tubular morphology [34], and two-dimensional graphene-based materials [35], which generally consist of nanosheets. Other well-known examples include nano-onions (CNOs) [36], which consist of concentric fullerenes, and nanohorns (CNHs), which arise from clusters of nanocones [37]. In recent years, the class of carbon dots has attracted attention thanks to their ultrasmall structure (<10 nm), which provides them with characteristic luminescent properties [38].

Carbon nanostructures have found a wide variety of applications over the years thanks to their electronic and thermal conductivity, low density, and high mechanical strength, as well as the ability to undergo chemical functionalization to further tune their properties as needed for the intended use [39]. They are being studied especially for energy [40] and catalysis [41–43], including electro-catalysis [44,45] and nanozymes [46], as well as for the development of advanced electronic applications [47], including supercapacitors [48,49] and batteries [50], wearable electronics [51], electro-catalytic water-splitting [52], electromagnetic interference (EMI) shielding materials [53], molecular magnets [54], thermal-energy harvesting [55], photo-detectors [56], and electrochemical sensors [57]. In particular, in the area of sensing [58], recent developments have been made in the areas of nano-mass and nano-force sensors [59], gas sensors [60], biosensors [61], temperature sensors [62], and the growing field of touch or motion-driven sensors, or “haptics” [63]. Another area of growing interest regards environmental remediation [64], including water purification [65] and the detection of various pollutants, such as pesticides [66] and pharmaceuticals [67].

In materials science, they are well-known as nano-fillers [68,69], but also used as flame-retardants [70].

Finally, carbon nanomaterials can be applied for biomedical use [71–74], especially in oncology [75,76], theranostics [77], drug delivery [78], antimicrobials [79,80], and DNA analysis [81]. A biomedical area that is progressing at a fast pace is tissue engineering [82], especially for nerve [83], cardiac [84], and bone [85] tissues. In bioelectronics, synaptic transistors and neuromorphic computing [86] are progressing at a fast pace.

2. Carbon Nanostructures as Templates for Titania Nanomorphologies

The efficiency of titania photo-activity can be significantly improved through nanostructuring and heterostructuring with carbon nanomaterials, allowing the enhanced use of the solar spectrum and better charge separation [87]. The addition of carbon nanostructures can lead to an increase of the adsorption capacity, of the absorption of visible light, and of the lifetime of photogenerated electron–hole pairs. In particular, CNTs have been widely used as supports for the growth of nanosized titania. The advantages of interfacing TiO_2 with CNTs include not only improved structural stability, but also electronic communication between the two phases, whereby charge carriers (electrons or holes) may be transferred through the phase boundaries through several proposed mechanisms. For instance, a general view is that CNTs can efficiently scavenge the titania photoexcited electrons, thus retarding the electron–hole recombination rates and resulting in enhanced photocatalytic activities [88]. It is worth noting, however, that alternative hypotheses have been advanced; for example, on the basis of transient absorption experiments, where the photogenerated holes are transferred from the TiO_2 to the CNT [89], confirming the complexity of the electron transfer dynamics, which for example could depend on the level of functionalization (in particular, with oxygenated groups) of the CNT surface. Other reports have suggested that CNTs can act as photosensitizers, with the electrons excited and injected from the CNTs into the TiO_2 conduction band, with subsequent electron transfer from the titania valence band into the CNTs, thus yielding a charge separation state (electron–hole) on the metal oxide. However, such sensitization effects assume a semiconducting character of the CNT, which cannot always be taken for granted. In general, the micro-structure of the CNT and its functional group distribution, doping, and method of preparation deeply affect the photochemical response. Furthermore, Ti–C and Ti–O–C bonds can be formed during calcination, thus resulting in a “doping” effect with the formation of intragap states within the titania and a consequent improved absorption of visible light [88].

The use of carbon nanomaterials to template titania with nanomorphological control was reviewed in 2016 [90]; thus, we focus here on the progresses made over the last five years. An overview of selected examples is provided in Table 1. A summary of the physicochemical properties of carbon nanostructures after decoration with titania, including the type of surface functionalization used to anchor the metal oxide, is provided in Table 2.

Carbon nanodots are not present in the table since they are typically not used as templates; rather, they are added onto preformed titania, for instance on anodized nanotube arrays for uses in photocatalysis [91] and sensing [92]. Readers with a particular interest in graphene quantum dots incorporated in titania nanostructures are referred elsewhere [93]. Furthermore, studies that used commercially available titania nanoparticles are not included, since our focus is on the influence of carbon nanomaterials on their formation.

Table 1. Overview of the use of different carbon nanomaterials as templates for nanostructured titania over the last five years.

Carbon Nanostructure	Titania Precursor	Titania Phase	Preparation Method	Titania Morphology	Application	Ref.
Fullerenol	Ti(OiPr) ₄	Amorphous	ALD ¹	Spherical	Photocatalysis	[94]
Nano-onions	Ti(OiPr) ₄	Anatase	Sol-gel	Irregular	Photocatalysis	[95]
Nano-onions	Ti(OiPr) ₄	Anatase	Sol-gel	Nanocrystals	Battery anode	[96]
Nano-onions	Ti(OiPr) ₄	Anatase	Hydrothermal	Nanocrystals	Supercapacitors	[97]
Nanocones	Ti(Obu) ₄	Anatase	Sol-gel	Nanocones@TiO ₂ ²	Photocatalysis	[98]
Nanohorns	Ti(Obu) ₄	Amorphous	Sol-gel	Nanohorns@TiO ₂ ²	Electrocatalysis	[99]
Nanohorns	Ti(Obu) ₄	Anatase	Solvothermal	Nanoflower	Photocatalysis	[100]
Nanohorns	Ti(OiPr) ₄	Anatase	Solvothermal	Nanohorns	Phosphoproteomics	[101]
Nanodiamonds	TiOSO ₄	Anatase	Hydrothermal	Irregular	Photocatalysis	[102]
Nanodiamonds	TiOSO ₄	Anatase	Hydrothermal	Nanocrystals	Photocatalysis	[103]
Nanodiamonds	(NH ₄) ₂ TiF ₆	Anatase	Hydrothermal	Nanocrystals	Photocatalysis	[104]
Nanodiamonds	Ti(Obu) ₄	Anatase/Brookite	Hydrothermal	Spherical	Battery anode	[105]
SWCNTs ³	Ti(Obu) ₄	Anatase/Rutile	Sol-gel	Nanocrystals	Photocatalysis	[106]
SWCNTs-C ₆₀ ^{3,4}	Ti(OiPr) ₄	n.a.	Sol-gel	CNT@C ₆₀ @TiO ₂ ²	Photocatalysis	[107]
MWCNTs ⁵	Ti(OiPr) ₄	Anatase	ALD ¹	CNT@TiO ₂ ²	Battery	[108]
MWCNTs ⁵	Ti(OiPr) ₄	Anatase	Sol-gel	Nanocrystals	Solar cells	[109]
MWCNTs ⁵	Ti(OiPr) ₄	Anatase	Sol-gel	Spherical	Photocatalysis	[110]
MWCNTs ⁵	Ti(OiPr) ₄	Anatase	Hydrothermal	Spherical	Nanofiller	[111]
MWCNTs ⁵	Ti(OiPr) ₄	Anatase	Hydrothermal	Spherical	Battery anode	[112]
MWCNTs ⁵	Ti(OiPr) ₄	Rutile	Hydrothermal	Flowers	Photocatalysis	[113]
MWCNTs ⁵	Ti(OiPr) ₄	Rutile	Hydrothermal	Nanorods	Photocatalysis	[114]
MWCNTs ⁵	Ti(OiPr) ₄	Rutile	Hydrothermal	Nanorods	Memory device	[115]
MWCNTs ⁵	Ti(OiPr) ₄	Anatase	Solvothermal	CNT@TiO ₂ ²	Electrocatalysis	[116]
MWCNTs ⁵	Ti(OiPr) ₄	Anatase	Solvothermal	Spherical	Battery anode	[117]
MWCNTs ⁵	Ti(OiPr) ₄	Anatase	Solvothermal	Nanorods	Phosphoproteomics	[101]
MWCNTs ⁵	Ti(OiPr) ₄	Anatase/Rutile	Electrospinning	Nanofibers	Solar cells	[118]
MWCNTs ⁵	Ti(Obu) ₄	Anatase	Sol-gel	Spherical	Battery anode	[119]
MWCNTs ⁵	Ti(Obu) ₄	Anatase	Sol-gel	CNT@TiO ₂ ²	Battery anode	[120]
MWCNTs ⁵	Ti(Obu) ₄	Anatase	Sol-gel	CNT@TiO ₂ ²	Photocatalysis	[121]
MWCNTs ⁵	Ti(Obu) ₄	Anatase/Rutile	Sol-gel	CNT@TiO ₂ ²	Microwave absorber	[122]
MWCNTs ⁵	Ti(Obu) ₄	Rutile	Sol-gel	CNT@TiO ₂ ²	Solar cells	[123]
MWCNTs ⁵	Ti(Obu) ₄	Anatase/Rutile	Sol-gel	Nanocrystals	Photocatalysis	[124]
MWCNTs ⁵	Ti(Obu) ₄	n.a.	Sol-gel	CNT@TiO ₂ ²	Electronics	[125]
MWCNTs ⁵	Ti(Obu) ₄	Anatase	Hydrothermal	Nanowires	Battery anode	[126]
MWCNTs ⁵	Ti(Obu) ₄	Anatase	Hydrothermal	Spherical	Battery anode	[127]
MWCNTs ⁵	Ti(Obu) ₄	Anatase	Hydrothermal	Nanosheets	Photocatalysis	[128]
MWCNTs ⁵	Ti(Obu) ₄	Rutile	Hydrothermal	Nanorods	Photocatalysis	[129]
MWCNTs ⁵	Ti(Obu) ₄	Anatase	Solvothermal	Flower	Battery anode	[130]

Table 1. Cont.

Carbon Nanostructure	Titania Precursor	Titania Phase	Preparation Method	Titania Morphology	Application	Ref.
MWCNTs ⁵	Ti(Obu) ₄	Anatase/Brookite	Solvothermal	Nanosheets	Battery anode	[131]
MWCNTs ⁵	Ti(Obu) ₄	Anatase/Brookite	Thermal	Spherical	Photocatalysis	[132]
MWCNTs ⁵	Ti(Obu) ₄	Anatase	Impregnation	Nanotubes	Battery cathode	[133]
MWCNTs ⁵	Ti(Obu) ₄	Anatase	Impregnation	CNT@TiO ₂ ²	Battery cathode	[133]
MWCNTs ⁵	Ti(OEt) ₄	Anatase/Rutile	Electrospinning	CNT@TiO ₂ ²	Photocatalysis	[89]
MWCNTs ⁵	TiOSO ₄	Anatase/Rutile	Solvothermal	Nanosheets	Photocatalysis	[134]
MWCNTs ⁵	PTO ⁶	Anatase/Brookite	Hydrothermal	Nanohorns	Battery anode	[135]
MWCNTs ⁵	Ti foil	Anatase	Micro-arc oxidation	Nanoflakes	Battery anode	[136]
MWCNTs ⁵	TiCl ₄	Anatase	Solvothermal	CNT@TiO ₂ ²	Photocatalysis	[137]
MWCNTs ⁵	TiCl ₄	Anatase	ALD ¹	CNT@TiO ₂ ²	Photocatalysis	[138]
MWCNTs ⁵	TDMAT ⁷	Anatase	ALD ¹	Films	Sensing	[139]
MWCNTs ⁵	TDMAT ⁷	<i>n.a.</i>	ALD ¹	CNT@TiO ₂ ²	Supercapacitors	[140]
CNT fibers	TDMAT ⁷	Anatase	ALD ¹	CNTbundle@TiO ₂ ²	Photoelectrode	[141]
CNT fibers	TDMAT ⁷	Anatase	ALD ¹	CNTbundle@TiO ₂ ²	Photoelectrode	[142]
MWCNTs-GO ⁸	Ti(OiPr) ₄	<i>n.a.</i>	Sol-gel	Irregular	Electrocatalysis	[143]
MWCNTs-GO ⁸	Ti(OiPr) ₄	<i>n.a.</i>	CVD ⁹	Irregular	Electrocatalysis	[143]
Graphene	Ti(OiPr) ₄	Anatase	Sol-gel	Nanocrystals	Photocatalysis	[144]
Graphene	Ti(OiPr) ₄	Anatase	Hydrothermal	GO@TiO ₂ ^{2,8}	Biosensing	[145]
Graphene	Ti(Obu) ₄	Anatase	Hydrothermal	Nanosheets	Photocatalysis	[146]
Graphene	Ti(Obu) ₄	Anatase	Hydrothermal	Nanocrystals	Photocatalysis	[147]
Graphene	Ti filament	Anatase	Sublimation	Spherical	Photocatalysis	[148]
Graphene	Ti	Amorphous	Electron beam	Film	Photocatalysis	[149]
GO ⁸	Ti(OiPr) ₄	Anatase	Solvothermal	Nanocrystals	Phosphoproteomics	[101]
GO ⁸	Ti(OiPr) ₄	Anatase	Laser scribing	Nanocrystals	Supercapacitors	[150]
GO ⁸	Ti(Obu) ₄	Anatase	Hydrothermal	Nanocrystals	Electrocatalysis	[151]
GO ⁸	Ti(Obu) ₄	Anatase	Hydrothermal	Nanocrystals	Battery anode	[152]
GO ⁸	Ti(Obu) ₄	Anatase/Brookite	Thermal	Spherical	Photocatalysis	[132]
GO ⁸	TiCl ₄	Anatase	Hydrothermal	GO@TiO ₂ ^{2,8}	Photocatalysis	[153]
GO ⁸	TiCl ₄	Rutile	Hydrothermal	Nanorods	Nanofiller	[154]
GO ⁸	Ti foil	Anatase	Anodization	Nanotubes	Supercapacitors	[155]
rGO ¹⁰	Ti(OiPr) ₄	Anatase	Sol-gel	Nanoparticles	Photocatalysis	[156]
rGO ¹⁰	Ti(OiPr) ₄	Anatase	Sol-gel/thermal	rGO@TiO ₂ ^{2,10}	Photocatalysis	[157]
rGO ¹⁰	Ti(OiPr) ₄	Anatase	Hydrothermal	rGO@TiO ₂ ^{2,10}	Photocatalysis	[158]
rGO ¹⁰	Ti(OiPr) ₄	Anatase	Hydrothermal	Nanocrystals	Sensing	[159]
rGO ¹⁰	Ti(OiPr) ₄	Anatase	Hydrothermal	Spherical	Battery anode	[112]
rGO ¹⁰	Ti(OiPr) ₄	Anatase	Hydrothermal	rGO@TiO ₂ ^{2,10}	Water purification	[160]
rGO ¹⁰	Ti(OiPr) ₄	Anatase	Solvothermal	rGO@TiO ₂ ^{2,10}	Photocatalysis	[161]
rGO ¹⁰	Ti(Obu) ₄	Anatase	Sol-gel	Nanoplatelets	Photocatalysis	[162]

Table 1. Cont.

Carbon Nanostructure	Titania Precursor	Titania Phase	Preparation Method	Titania Morphology	Application	Ref.
rGO ¹⁰	Ti(OBu) ₄	Anatase	Sol-gel	rGO@TiO ₂ ^{2,10}	Photoelectrocatalysis	[163]
rGO ¹⁰	Ti(OBu) ₄	Anatase/Rutile	Sol-gel	rGO@TiO ₂ ^{2,10}	Photocatalysis	[164]
rGO ¹⁰	Ti(OBu) ₄	Rutile/Brookite	Sol-gel	Nanocrystals	Photocatalysis	[165]
rGO ¹⁰	Ti(OBu) ₄	Anatase	Hydrothermal	rGO@TiO ₂ ^{2,10}	Photocatalysis	[166]
rGO ¹⁰	Ti(OBu) ₄	Anatase	Hydrothermal	rGO@TiO ₂ ^{2,10}	Photocatalysis	[167]
rGO ¹⁰	Ti(OBu) ₄	Anatase	Hydrothermal	Spherical	Photocatalysis	[168]
rGO ¹⁰	Ti(OBu) ₄	Anatase	Solvothermal	Nanocrystals	Lubrication	[169]
rGO ¹⁰	Ti(OBu) ₄	Amorphous	Solvothermal	Nanorods	Microwave absorber	[170]
rGO ¹⁰	Ti(OBu) ₄	Anatase	Electrospinning	rGO@TiO ₂ ^{2,10}	Photocatalysis	[171]
rGO ¹⁰	TiCl ₄	Anatase	Hydrothermal	Irregular	Photocatalysis	[172]
rGO ¹⁰	TiCl ₃	Anatase	Microwave	Spherical	Battery anode	[173]
Nano-graphite	Ti(OiPr) ₄	Anatase/Rutile	ALD ¹	graphite@TiO ₂ ²	Photocatalysis	[174]

¹ ALD = atomic layer deposition. ² @ denotes core@shell structure. ³ SWCNTs = single-walled carbon nanotubes. ⁴ C₆₀ is a fullerene with 60 carbon atoms. ⁵ MWCNTs = multi-walled carbon nanotubes. ⁶ PTO = potassium titanium oxide oxalate. ⁷ TDMAT = tetrakis (dimethylamino)titanium. ⁸ GO = graphene oxide. ⁹ CVD = chemical vapor deposition. ¹⁰ rGO = reduced graphene oxide. Ti(OiPr)₄ = titanium (IV) isopropoxide. ti(OBu)₄ = titanium (IV) butoxide. TiOSO₄ = titanium (IV) oxysulfate. (NH₄)₂TiF₆ = ammonium hexafluorotitanate. Ti(OEt)₄ = Titanium (IV) ethoxide.

Table 2. Summary of the physicochemical properties of carbon nanostructures decorated with titania over the last five years.

Carbon Nanostructure (CN)	Nanocarbon Surface Functionalization	Distinctive Raman Peaks (cm ⁻¹)	Specific Surface Area (m ² g ⁻¹)	TiO ₂ Crystallite Size (nm)	Ref.
Fullerenol	OH	1465 (CN)	<i>n.a.</i>	<i>n.a.</i>	[94]
Nano-onions	Oxidation	<i>n.a.</i>	263	<i>n.a.</i>	[95]
Nano-onions	<i>n.a.</i>	143, 195, 396, 518, 639 (A) ¹	<i>n.a.</i>	<10	[96]
Nano-onions	<i>n.a.</i>	146, 370, 490, 610 (A) ¹ 1338, 1574 (CN)	101–148	9–10	[97]
Nanocones	Oxidation	Anatase, D and G bands (CN)	126	11	[98]
Nanohorns	Oxidation	D and G bands (CN)	148	<i>n.a.</i>	[99]
Nanohorns	<i>n.a.</i>	138, 386, 506, 629 (A) ¹ 1336, 1568 (CN)	<i>n.a.</i>	9	[100]
Nanohorns	Oxidation, magnetization	Anatase, D and G bands (CN)	38	<i>n.a.</i>	[101]
Nanodiamonds	Oxidation	148, 398, 516, 636 (A) ¹ 1324 (CN)	77	<5	[102]
Nanodiamonds	Oxidation	152, 397, 516, 644 (A) ¹ 1324, 1400–1700 (CN)	232–252	4	[103]
Nanodiamonds	Pristine/COOH/NH ₂ /CH	<i>n.a.</i>	60–102	9–10	[104]
Nanodiamonds	Oxidation	<i>n.a.</i>	153	4	[105]
SWCNTs ²	SDBS ³ (non-covalent)	Anatase, rutile RBM, D, G bands (CN)	293	9	[106]

Table 2. Cont.

Carbon Nanostructure (CN)	Nanocarbon Surface Functionalization	Distinctive Raman Peaks (cm ⁻¹)	Specific Surface Area (m ² g ⁻¹)	TiO ₂ Crystallite Size (nm)	Ref.
SWCNTs-C ₆₀ ^{2,4}	Fullerodendron	425, 610 (titania) 1139, 1610 (CN)	<i>n.a.</i>	<i>n.a.</i>	[107]
MWCNTs ⁵	Pristine/ oxidation/N-doping	143 (A) ¹ D and G bands (CN)	<i>n.a.</i>	5–10	[108]
MWCNTs ⁵	Oxidation	145, 398, 517, 641 (A) ¹ 1351, 1582 (CN)	60–110	15–19	[109]
MWCNTs ⁵	Oxidation	<i>n.a.</i>	104–190	9–17	[110]
MWCNTs ⁵	OH	1342, 1576 (CN)	<i>n.a.</i>	<i>n.a.</i>	[111]
MWCNTs ⁵	SDS ⁶ (non-covalent)	<i>n.a.</i>	50	14	[113]
MWCNTs ⁵	Oxidation	234, 432, 612 (R) ⁷ 1358, 1580, 2711 (CN)	187–249	<i>n.a.</i>	[114]
MWCNTs ⁵	SDS ⁶ (non-covalent)	448, 611 (R) ⁷ 1355, 1600 (CN)	<i>n.a.</i>	6–7	[115]
MWCNTs ⁵	OH	161, 388, 516, 634 (A) ¹ 1338, 1578, 2673 (CN)	170	23	[117]
MWCNTs ⁵	Oxidation, magnetization	Anatase, D and G band (CN)	30	<i>n.a.</i>	[101]
MWCNTs ⁵	PVP ⁸ -PAN ⁹ (non-covalent)	143 (A) ¹ , 245, 421, 602 (R) ⁷ 1325, 1592 (CN)	276	<i>n.a.</i>	[118]
MWCNTs ⁵	Ammonia treatment	153, 202, 394, 207, 512, 631 (A) ¹ D and G bands (CN)	<i>n.a.</i>	6	[119]
MWCNTs ⁵	<i>n.a.</i>	Anatase, D and G bands (CN)	221	2	[120]
MWCNTs ⁵	Benzoic acid	146, 198, 395, 513, 639 (A) ¹ D, G, 2D bands (CN)	222–228	10	[121]
MWCNTs ⁵	Oxidation	153, 396, 513, 635 (A) ¹ 1329, 1597 (CN)	<i>n.a.</i>	<i>n.a.</i>	[122]
MWCNTs ⁵	N-doping, acid treatment	<i>n.a.</i>	160–295	10	[123]
MWCNTs ⁵	Oxidation	<i>n.a.</i>	<i>n.a.</i>	15	[124]
MWCNTs ⁵	OH	Anatase, D and G bands (CN)	<i>n.a.</i>	<i>n.a.</i>	[126]
MWCNTs ⁵	<i>n.a.</i>	142, 446, 610 (R) ⁷ 1365, 1591 (CN)	<i>n.a.</i>	<i>n.a.</i>	[129]
MWCNTs ⁵	Oxidation	<i>n.a.</i>	71–266	<i>n.a.</i>	[130]
MWCNTs ⁵	<i>n.a.</i>	Anatase, 1342 and 1574 (CN)	62–115	8	[131]
MWCNTs ⁵	Oxidation	144, 515, 640 (A) 1356, 1591, 1754, 1775, 2704 (CN)	440	<i>n.a.</i>	[132]
MWCNTs ⁵	Oxidation	<i>n.a.</i>	137	5–6	[133]
MWCNTs ⁵	Oxidation, PVP ⁸	144, 197, 399, 515, 519, 639 (A) ¹ 447 and 612 (R) ⁷ 1345 and 1594 (CN)	<i>n.a.</i>	12	[89]
MWCNTs ⁵	<i>n.a.</i>	<i>n.a.</i>	244	5–10	[134]
MWCNTs ⁵	Oxidation	149, 199, 390, 512, 639 (A) ¹ 289 (B) ¹⁰ , 1346 and 1578 (CN)	80–102	<i>n.a.</i>	[135]
MWCNTs ⁵	Oxidation	394, 515, 636 (A) ¹ 1352 and 1585 (CN)	<i>n.a.</i>	<i>n.a.</i>	[136]

Table 2. Cont.

Carbon Nanostructure (CN)	Nanocarbon Surface Functionalization	Distinctive Raman Peaks (cm ⁻¹)	Specific Surface Area (m ² g ⁻¹)	TiO ₂ Crystallite Size (nm)	Ref.
MWCNTs ⁵	OH	146, 396, 513, 637 (A) ¹ 1331 and 1581 (CN)	85–103	5–7	[137]
MWCNTs ⁵	Oxidation	146, 395, 515, 635 (A) ¹ 1347 and 1582 (CN)	<i>n.a.</i>	<i>n.a.</i>	[138]
MWCNTs ⁵	Carboxyl plasma polymer	144–149 (A) ¹ 1340, 1580, 2685 (CN)	<i>n.a.</i>	<i>n.a.</i>	[139]
CNT fibers	Oxidation	147, 199, 395, 514, 636 (A) ¹ 1344, 1578, 1620, 2681 (CN)	<i>n.a.</i>	< 10	[141]
MWCNTs-GO ¹⁰	N-doping	1350, 1580 (CN)	135–417	<i>n.a.</i>	[143]
Graphene	<i>n.a.</i>	Anatase, D, G, 2D bands (CN)	88–136	9–12	[144]
Graphene	Oxidation	159, 636 (A) ¹ 1333, 1698 (CN)	<i>n.a.</i>	2	[147]
GO ¹⁰	Magnetization	Anatase, D and G bands (CN)	45	9–17	[101]
GO ¹⁰	<i>n.a.</i>	155 (A) ¹ , 1370 and 1600 (CN)	<i>n.a.</i>	5	[150]
GO ¹⁰	N-doping	1340, 1590 (CN)	<i>n.a.</i>	2	[151]
GO ¹⁰	Oxidation	145, 398, 517, 629 (A) ¹ 1331, 1599 (CN)	<i>n.a.</i>	<i>n.a.</i>	[152]
GO ¹⁰	<i>n.a.</i>	144, 515, 640 (A) 193, 244, 272, 321, 362, 434 (B) ¹¹ 1357, 1600, 1670 (CN)	459	<i>n.a.</i>	[132]
GO ¹⁰	<i>n.a.</i>	397, 518 (A) ¹ 1350, 1570, 1620, 2600 (CN)	<i>n.a.</i>	1.5	[153]
GO ¹⁰	CS ¹² , PVA ¹³ (non-covalent)	444, 608 (R) ⁷ 1351, 1601 (CN)	<i>n.a.</i>	<i>n.a.</i>	[154]
GO ¹⁰	Adenine	147, 159, 402, 513, 635 (A) ¹ 1354, 1576 (CN)	<i>n.a.</i>	32	[155]
rGO ¹⁴	Erbium (impregnation)	458, 463, 616, 633 (A) ¹ 1353, 1598 (CN)	53	10	[156]
rGO ¹⁴	<i>n.a.</i>	145, 398, 517, 640 (A) ¹ 1354, 1584 (CN)	78	<i>n.a.</i>	[157]
rGO ¹⁴	<i>n.a.</i>	150, 394, 510, 629 (A) ¹ D and G bands (CN)	119	15	[158]
rGO ¹⁴	<i>n.a.</i>	319 and 515 (A) ¹ 1330 and 1604 (CN)	104	5	[112]
rGO ¹⁴	ZnS	150–153, 199, 639 (A) ¹ 1350, 1597 (CN)	441–460	15–24	[161]
rGO ¹⁴	<i>n.a.</i>	Anatase, 1359, 2578 (CN)	55	10	[162]
rGO ¹⁴	<i>n.a.</i>	144, 194, 395, 515, 636 (A) ¹ 1457, 1601 (CN)	<i>n.a.</i>	25	[163]
rGO ¹⁴	<i>n.a.</i>	145, 393, 638 (A) ¹ 445 (R) ⁷ 1323, 1570 (CN)	<i>n.a.</i>	23–36	[164]
rGO ¹⁴	<i>n.a.</i>	126, 146 (B) ¹¹ 452 (R) ⁷	51	<i>n.a.</i>	[165]
rGO ¹⁴	P-doped cellulose	600 (A) ¹ , 1350, 1580 (CN)	344	<i>n.a.</i>	[166]
rGO ¹⁴	Sm ₂ MoO ₆	1345, 1569 (CN)	<i>n.a.</i>	<i>n.a.</i>	[167]
rGO ¹⁴	<i>n.a.</i>	<i>n.a.</i>	102	20–30	[168]

Table 2. Cont.

Carbon Nanostructure (CN)	Nanocarbon Surface Functionalization	Distinctive Raman Peaks (cm ⁻¹)	Specific Surface Area (m ² g ⁻¹)	TiO ₂ Crystallite Size (nm)	Ref.
rGO ¹⁴	F-doping	146, 397, 516, 637 (A) ¹ 1354, 1596 (CN)	n.a.	15	[169]
rGO ¹⁴	n.a.	1343, 1590 (CN)	95	20	[172]

¹ A = anatase. ² SWCNTs = single-walled carbon nanotubes. ³ SDBS = sodium dodecylbenzene sulfonate. ⁴ C₆₀ is a fullerene with 60 carbon atoms. ⁵ MWCNTs = multi-walled carbon nanotubes. ⁶ SDS = sodium dodecyl sulfate. ⁷ R = rutile. ⁸ PyPBI = pyridine-based polybenzimidazole. ⁹ PVP = polyvinylpyrrolidone. ¹⁰ PAN = polyacrylonitrile. ¹¹ GO = graphene oxide. ¹² B = brookite. ¹³ CS = chitosan. ¹⁴ PVA = polyvinyl alcohol. ¹⁴ rGO = reduced graphene oxide.

2.1. Fullerenes

Fullerenes have been intensively studied for photocatalytic applications, as well as in combination with other semiconductors as photocatalyst enhancers [175]. The use of fullerenes as nano-templates for titania nucleation and growth was mainly developed in previous years [88], despite a modern renaissance of their use in solar cells [176].

Zinc-functionalized fullerene was recently combined with nanostructured titania for water remediation; however, the two nanomaterials were formed separately and only later combined to make nanostructured composites [177]. The interface between fullerenes and titania has been deeply investigated. It was recently found that defect states in the band gap of titania are quenched by C₇₀ while an interfacial state appears, showing a barrier-free extraction of charges (Figure 3) for the next generation of organic solar cells [178]. However, in studies such as this one, fullerenes are added onto preformed titania.

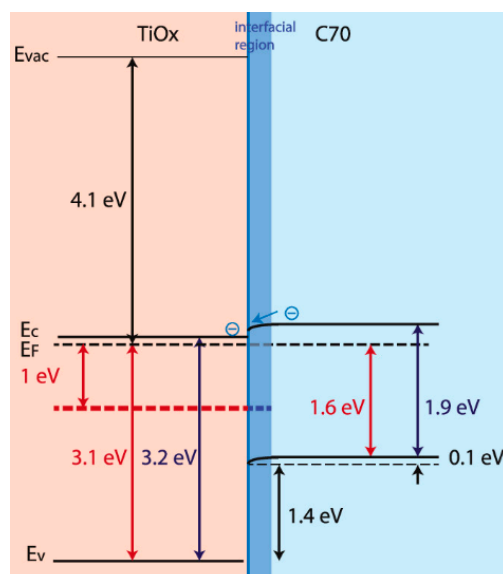


Figure 3. C₇₀/titania band diagrams derived from the photoemission spectra, with energy gaps based on optical absorption data. Reproduced with permission from [178], copyright © 2021, American Chemical Society.

In an interesting study, fullerenol was used as a template for titania to exploit the buckyball's hydroxyl groups as nucleation sites for the generation of titania nanoparticles by atomic layer deposition using titanium tetraisopropoxide as a precursor [94]. Given the low temperatures used in the process, the resulting titania was amorphous, yet it surprisingly demonstrated photocatalytic activity that was ascribed to the presence of fullerene in the composite material [94].

2.2. Nano-Onions

Carbon nano-onions consist of concentric fullerenes and have been used usually to template nanostructured titania by means of sol-gel methods. X-ray diffraction analyses confirmed that the nanocarbons were anchored onto anatase, whose microscopy images suggested a certain level of control against the particle agglomeration exerted by the nano-onions, relative to a reference without the template, despite the limited morphological control over the titania particles. The nano-onions enhanced the specific surface area, average pore size, and pore volume of the composite leading to the adsorption of pollutants, as well as its visible-light absorption, overall leading to a more efficient photocatalytic dye degradation as demonstrated on rhodamine B. Finally, the paramagnetic nature of the nano-onions with a magnetic core allowed for the easy recovery of the composite through magnetic separation [95].

Carbon nano-onion/anatase hybrids have been proposed as innovative replacements for graphite anodes in lithium-ion batteries. Titania was formed with a sol-gel method onto the nanocarbon template, exerting a certain level of both morphological and size control over the nanocrystals, which appeared to be smaller than 10 nanometers in diameter. Furthermore, the presence of the conductive carbon nanostructure overall significantly enhanced the electrochemical properties of the final material relative to the reference without the nano-onions [96].

Carbon nano-onions/anatase materials were also obtained by a hydrothermal route, with various mass compositions, ranging from an excess of the nano-onion to an excess of the titania, as confirmed by thermogravimetric analyses. The best results within the series were obtained with compositions featuring approximately 80–90 wt% nano-onions. In particular, high-resolution transmission electron microscopy (HR-TEM) images (Figure 4) revealed an intimate contact between the inorganic and the carbon components, with both the graphitic walls of the nano-onions and the lattice of the anatase nanocrystals being clearly visible. These materials demonstrated the highest capacitance and an enhanced electrochemical performance overall, which was rationalized through a cooperative effect of both the electrochemical double layer capacitance from the nano-onions and non-capacitive Faradaic storage regarded as pseudocapacitance from titania [97]. Carbon nano-onions have been proposed for use in dye-sensitized solar cells, thanks to a number of advantageous features, including their limited cost, ease of dispersibility that does not require the use of binders—in contrast with other carbon nanomaterials—and the high level of optical transparency of the final device [179].

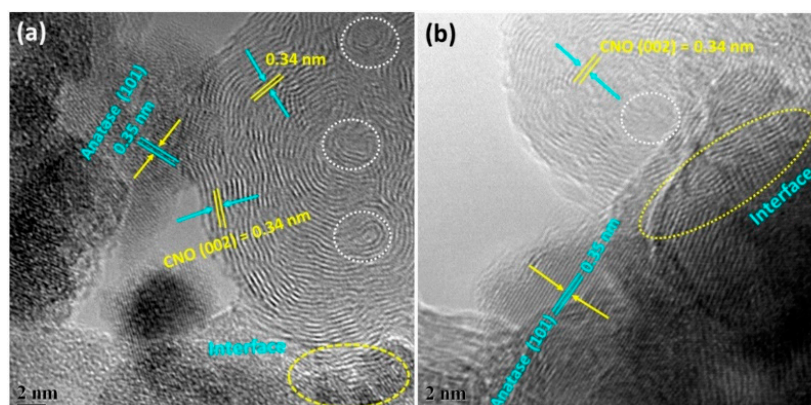


Figure 4. HR-TEM images of carbon nano-onion/anatase nanocrystals with different ratios of the two components, consisting of either (a) 89 wt%/11 wt% or (b) 83 wt%/17 wt%, respectively. White-dotted circles highlight the nano-onion cores; yellow-dotted circles indicate the interface between the two components. The nano-onion graphitic walls area visible with the typical 0.34 nm-distance, as is the lattice spacing of 0.35 nm, corresponding to the (101) plane of anatase. Reprinted from [97], Copyright © 2017, with permission from Elsevier.

2.3. Nanocones

The cone-like morphology of carbon nanocones leads to very interesting features, such as an uncommon graphene-sheet stacking depending on the apex (cone) angle, which in turn implies the presence of a number of pentagons within the six-membered ring patterns, creating the conical geometry. In the absence of pentagons, the angle can reach 0° , thus resulting in a flat disk. Nanocones are normally produced as a mixture of these varied structures with differing geometrical parameters and containing a large excess (approximately 70%) of disks. The nanocones were oxidized to display hydroxyl groups that could act as anchor sites for the inorganic phase, which was grown as a uniform coating reproducing the nanocone morphology with high fidelity through a sol-gel process. The coating included embedded palladium nanoparticles, and the final material displayed very high photocatalytic activity under UV irradiation thanks to an increased surface area and the ability of the carbon framework to scavenge the photo-excited electrons to retard the charge recombination rates. Despite the lower conductivity relative to carbon nanotubes or graphene, nanocones provide other advantages, such as the ease of dispersibility in liquid media. The intimate contact between the organic and the inorganic phases, leading to an increased number of heterojunctions, was responsible for the higher activity in photocatalytic hydrogen production, using ethanol as an environmentally friendly sacrificial donor, which is conveniently a product of fermentation from feedstock (corn, sugarcane, etc.) [98].

2.4. Nanohorns

Nanohorns can be considered as clusters of nanocones, and they have also been used as templates for titania. The nanocarbon entanglement features a high surface area that templates a large distribution of “hard-soft” bimetallic sites, where 1.5 nm palladium nanoparticles were embedded within the titania phase while being electrically wired to an electrode by the nanohorn support. This hybrid electrocatalyst activated carbon dioxide reduction to formic acid nearly at zero overpotential in the aqueous phase, while being able to produce hydrogen thanks to a sequential formic acid reduction [99].

In another study, nanohorns templated the formation of anatase with nanoflower morphology through a solvothermal method. The photocatalytic degradation of two model dyes (i.e., methylene blue and methyl orange) was combined with the generation of hydrogen fuel upon solar-light irradiation [100].

Besides the prospective uses in solar cells [180,181], nanohorns are potentially suitable for biological uses thanks to their additional advantageous features relative to other carbon nano-allotropes, such as the ease of oxidation and the high dispersibility in buffer solutions [182]. To this end, they have been used as templates for nanostructured titania with the nanohorn morphology and applied to phosphoproteomics on cancer cell lysates for diagnostics purposes thanks to the well-known binding affinity for titania with phosphorylated peptides (Figure 5) [101].

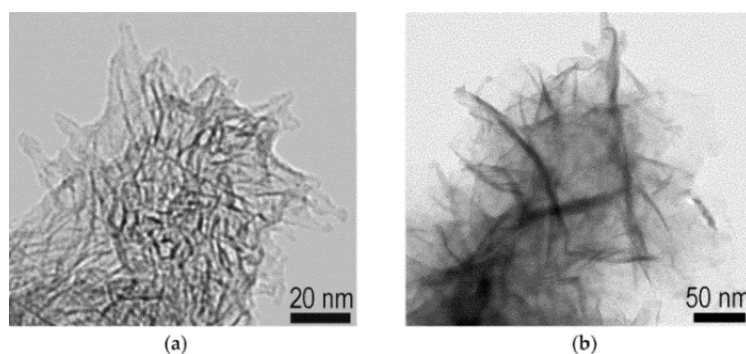


Figure 5. TEM images of carbon nanohorns (a) without or (b) with anatase [101].

2.5. Nanodiamonds

Nanodiamonds' high thermal conductivity, hardness and friction-resistance, high surface area, chemical inertness, non-toxicity, tunable structure, and excellent opto-mechanical properties have rendered them attractive building blocks in nanotechnology [183]. Nanodiamonds are typically produced by explosive detonation under oxygen-deficient conditions and consist of nanoparticles as small as 4–5 nm with a large portion of sp^3 -hybridized carbon atoms, in addition to sp^2 -hybridized atoms. A hydrothermal method at 70 °C was used as an easy and low-cost production method for the nucleation and growth of titania nanoparticles. Despite the limited control over the particle morphology and the presence of agglomerates, the presence of the nanodiamonds allowed for a reduced recombination rate of photogenerated charge carriers, with an improved photodegradation of bisphenol A as a model organic pollutant [102]. Similar protocols produced nanodiamonds–titania composites that were successfully tested for the photodegradation of other pollutants, thus confirming their versatility towards environmental remediation [103,104]. Further, this kind of nanomaterial has been envisaged as an anodic component for lithium batteries, thanks to the features of nanocarbon, such as its high lithium adsorption capacity, wide surface area, and chemical inertness, as well as its overall high capacitance and the long-term cycle stability of the composites [105].

2.6. Single-Walled Carbon Nanotubes (SWCNTs)

The use of SWCNTs is less common than MWCNTs due to the latter being easier to handle and disperse and presenting lower costs of production. In one study, SWCNTs successfully templated the formation of titania through a sol-gel method, and subsequent calcination at 600 °C allowed for the crystallization into anatase/rutile phases onto the tubes and the formation of an aerogel, which was tested for photocatalysis. The addition of platinum nanoparticles as co-catalysts onto the tubes, prior to titania nucleation and growth, was also studied to enhance the activity thanks to a more efficient charge carrier separation [106].

In another work, SWCNTs were first coated with a dendrofullerene (Figure 6) to provide suitable anchoring points for the nucleation and growth of titania while leading to good performance with regard to photo-catalytic H_2 evolution under visible-light irradiation. Co-axial inorganic–organic nanowires were thus obtained with a high photo-activity that was rationalized in terms of the electron-extracting TiO_2 layer accelerating the electron forward-transfer and the concomitant deceleration of the undesired back-transfer [107].

2.7. Multi-Walled Carbon Nanotubes (MWCNTs)

MWCNTs have been widely studied as templates for titania nanostructures, as can be seen from the many entries in Table 1; thus, only a few studies are discussed here. With a sol-gel process in ethanol using a tetrabutyl titanate precursor, it was possible to decorate CNTs with titania nanocrystals, and the materials were used to obtain a film for potential applications as a battery anode [119]. When the same precursor was used in alkaline aqueous solutions with wider, hydroxylated CNTs (average diameter of 50 nm), nanowires were obtained instead, which entangled with CNTs in a network and were envisaged for the same application [126]. The CNT/titanium relative ratio is one of the critical parameters that determines nanomorphology. For instance, when an excess of titania precursor was used in a solvothermal method, nanoflowers were obtained, while increasing the relative amount of CNTs yielded nanowires through which the titania anatase coated the CNTs [130].

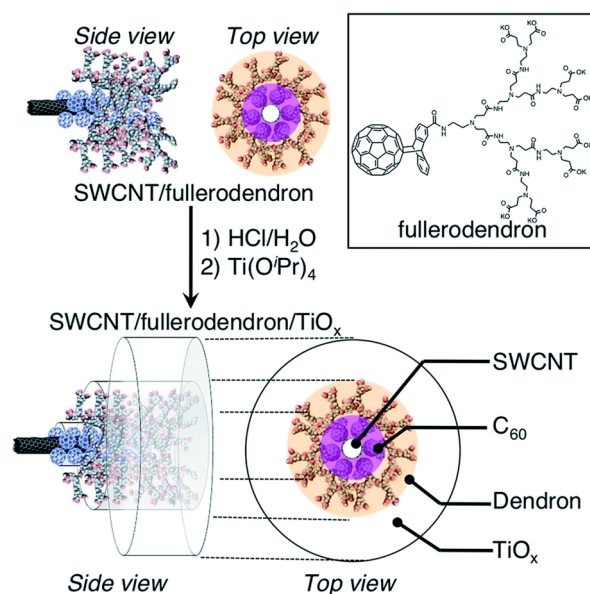


Figure 6. Schematic illustration of the fabrication of SWCNT/fullerodendron/titania co-axial hybrid nano-wires. Reproduced from [107], published by the Royal Society of Chemistry.

The hollow interior of MWCNTs can also be exploited for various functions. For instance, iron-filled nanotubes could harness a magnetic separation after use for the easy recovery of the photocatalytic system. The tubes were functionalized on their surface to display carboxylic acid groups as anchors for titania nucleation and growth, and a thermal treatment allowed for the formation of anatase nanocrystals on the surface of CNTs (Figure 7) [184].

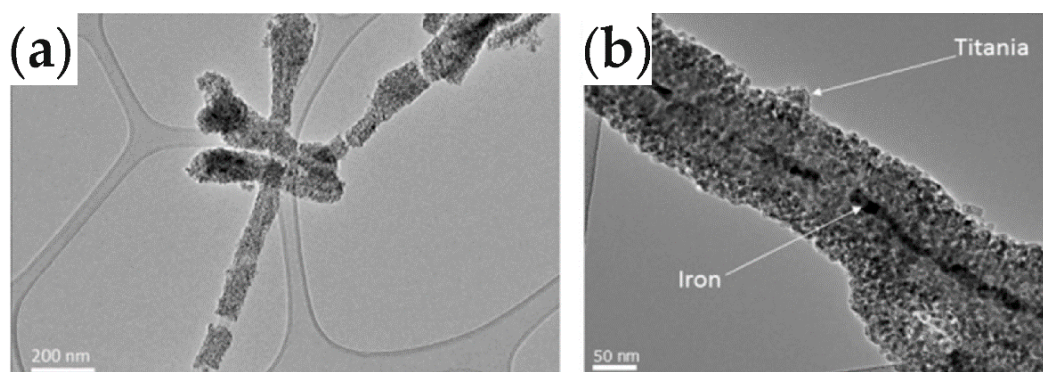


Figure 7. TEM images at lower (a) and higher (b) magnification show MWCNTs coated with titania nanocrystals and partially filled with iron inside for the magnetic separation and recovery of the photocatalyst after use. Reprinted from [184], Copyright © 2018, with permission from Elsevier.

2.8. Graphene, Graphene Oxide (GO) and Reduced Graphene Oxide (rGO)

The combination of graphene-based materials and titania is perhaps the most investigated nanocarbon-titania combination, and the topic was reviewed in 2017 [185] and 2019 [186]. Therefore, we focus here on the progresses made in the last two years and, given the vast amount of relevant literature, only selected examples are discussed in this section, while more can be found in Table 1.

Despite the sheet morphology of graphene-based materials, they can be used also to successfully attain elongated nanofibers, as demonstrated by the use of electrospinning techniques. This technique allows continuous nanofibers to be drawn from a liquid, thanks to electrostatic forces in the liquid jet that accelerates through an electric field.

The inclusion of both rGO and a titania precursor in the dispersion of reagents allowed electrospun nanofibers to be attained that after calcination revealed a shell anatase titania round a core with rGO. The nanofibrous exhibited the efficient photocatalytic degradation of a drug and a dye as model pollutants [171].

The enhanced photo-activity arises from synergistic effects, and it critically hinges on the covalent bonds between the two phases, which can be confirmed through the spectroscopic characterization of the Ti-O-C signature. To this end, it can be convenient to use titanium tetrachloride as a titania precursor, as the chloride is an excellent leaving group that can be replaced by the oxygen of the hydroxyl groups present on graphene [153].

Other important parameters that determine the performance of the final materials are clearly the crystallinity and particle size or film thickness of titania [187]. Solvothermal methods have been proven to be appropriate for attaining the complete coverage of graphene oxide flakes by highly homogeneous anatase nanocrystals (approximately 10–20 nm in size) (Figure 8a). In silico investigations confirmed that the presence of oxygen-bearing functional groups on graphene oxide acted as anchoring sites for the nucleation of anatase (Figure 8b–d), which was favored over the growth of larger crystals. Comparison with analogous composites obtained using different nanocarbons (i.e., MWCNTs, nanohorns, or graphitized carbon black), revealed that graphene-based material displayed the highest selectivity for phosphopeptides relative to non-phosphorylated peptides. The former could thus be enriched from cancer cell lysates for phosphoproteomics profiling, in a proof-of-concept study for oncological research and potentially for the early detection of cancer [101].

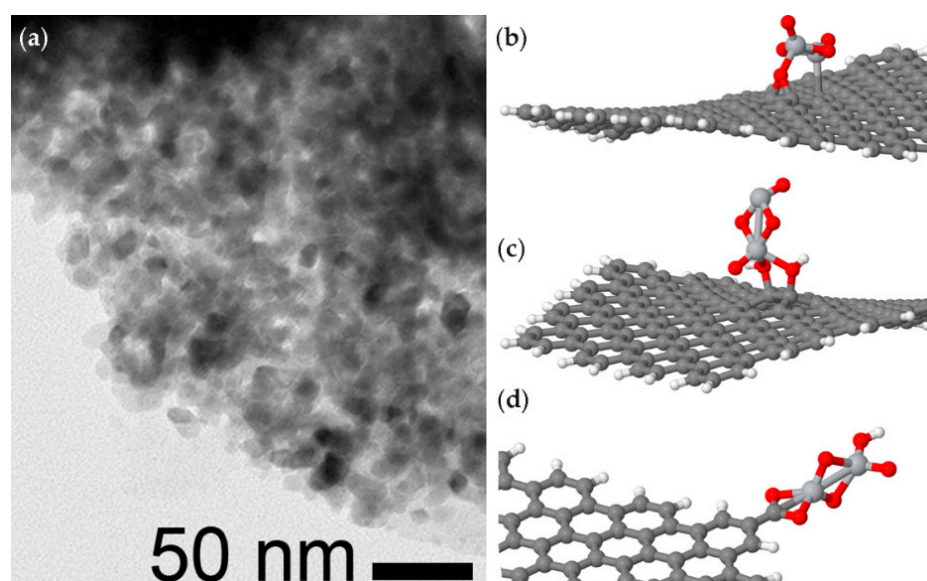


Figure 8. (a) TEM image of a graphene oxide flake covered by anatase titania nanocrystals that are highly homogeneous in size; (b–d) in silico investigation revealed how the nanocarbon’s oxygen-bearing functional groups (i.e., (b) epoxide, (c) hydroxyl, and (d) carboxylic acid) anchored titanium species, thus favoring nucleation over the growth of the nanocrystals. Adapted by permission from Springer Nature [101], copyright © 2020.

3. Applications

As mentioned in the introduction, nanostructured titania finds a wide variety of applications in areas spanning from energy to medicine, as described below more in detail.

3.1. Photocatalysis for Energy and Synthesis

Titania is a promising candidate for photocatalytic applications related to sustainable schemes for energy and environment. For instance, titania is well-studied for the conversion of carbon dioxide into a range of useful fuels or commodities, such as methane, methanol,

ethylene, formaldehyde, or formic acid [188]. For hydrogenation reactions, such as those of carbon dioxide and monoxide, titania and titanates have also been used as active supports for Rh catalysts [189]. Additionally, iridium-based catalysts have benefited from research that developed titania-based active supports for the photocatalytic synthesis of benzimidazoles, whereby rutile surpassed anatase in terms of performance, thanks to an increase in the adsorption of the reagents and in the charge transfer from the support, both of which led to higher product yields [190].

The photoelectrochemical generation of hydrogen from water has also enjoyed great prominence, where one-dimensional titania nanostructures demonstrated promising performance [191]. In silico tools are highly valuable to understand the nature of the rate-limiting steps and anticipate the better approaches to improve the efficiency of the process [192]. The further improvement of the photocatalytic performance of titania can be achieved through combination with other metal oxides (such as SnO_2 [193], ZnO [194], CuO [195]), gold [196,197], as well as alkali metals and conducting polymers [198], carbon-doping [199], iron oxides to attain magnetic systems [200], gadolinium [201], various rare earths [202], and bismuth vanadate [203], amongst others. In particular, the use of 4D transition metals was shown to be effective through the production of impurity-originating intra-gap energy states, but also through the semiconductor–metal phase transition [204].

A recent promising approach consists of single-atom doping. In the case of copper, light irradiation leads to electron transfer and the protonation of Cu/titania, and a local distortion around the copper atom stabilizes the deep-trap state on the copper d-orbital and its decoupling from free charges, thus yielding high photocatalytic hydrogen generation activity [205]. Further, the photocatalytic performance of Cu/titania can be improved by spin selection, which is achieved via optical intersite spin transfer or chiral semiconductor coating [205]. Both hydrogen adsorption and spin selection processes increase charge carrier lifetimes by an order of magnitude [205].

3.2. Photocatalysis for Environmental Remediation

The photoactivity of titania has been widely applied for environmental remediation; for instance, through the generation of graphene-bearing membranes for water purification [186,206]. The mechanisms of titania-photocatalyzed dye degradation proceed through the generation of reactive oxygen species (ROS) that trigger the photooxidation of organic molecules [207]. This phenomenon can be applied to a variety of different pollutants. They include dyes, for which titania co-doping with iron and praseodymium was recently reported to significantly narrow the band gap. Moreover, it promoted the generation of oxygen vacancies, which can trap electrons and thus reduce the recombination of charge carriers [208]. Nitrogen and sulfur co-doping represents a very popular strategy to enhance the photodegradation of cationic dyes [209]. Another type of target pollutants consists of volatile organics, whose photo-degradation is heavily influenced by levels of humidity [210]. Another area that requires urgent action is the environmental pollution by drugs, especially antibiotics, whose mechanisms of photodegradation are still the subject of intense investigations [211]. Clearly, the removal of pesticides is also highly sought after, although a number of variables have to be taken into consideration as they may affect the efficiency of the process [212]. Ammonia is a critical pollutant of agricultural concern, both in gaseous and aqueous matrices, for which heterogeneous nanostructures find application as photocatalysts [213]. In fact, ammonia splitting into nitrogen and hydrogen gases is particularly attractive as it would concomitantly generate clean fuel [214]. The fundamental reaction pathways involved in the process are shown in Figure 9 [214].

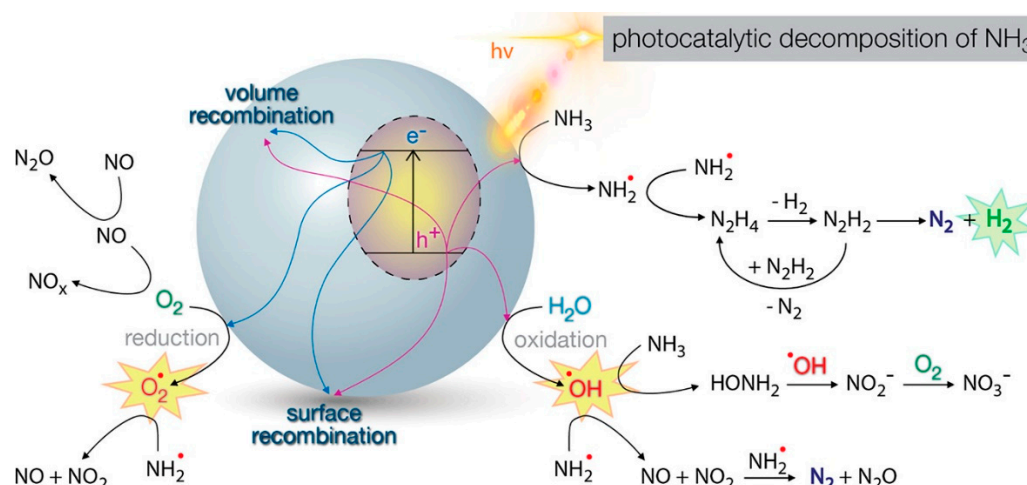


Figure 9. Scheme of the fundamental reaction pathways of ammonia degradation photocatalyzed by titania. Reprinted with permission from [214], Copyright © 2020, American Chemical Society.

Sometimes, different photoactive catalysts are combined together to enhance the performance of the final materials [215]. Alternatively, doping can be an effective strategy; for instance, with bismuth [216], tungsten [217], nickel [218], and so on.

3.3. Biomedical Applications and Public Health

The photoactivity of titania nanoparticles has also been recently investigated for applications in medicine. The most popular uses exploit the ability of nanostructured titania to generate ROS upon light irradiation, as these species can be employed for photodynamic therapy, but also for the inactivation of bacteria that are resistant to antibiotics [219]. Another area that is gaining momentum is the development of active coatings and films for food packaging [220]. To this end, the antimicrobial activity phototriggered by nanostructured titania can be boosted upon the inclusion of silver or copper species, for applications that go beyond food packaging, including also active textiles and self-cleaning fabrics [221].

Titania nanotubes are being investigated as vehicles for local drug delivery, especially if functionalized to promote osteogenesis at the bone–implant interface, as recently reviewed [222]. Given the widespread use of titanium implants, the possibility to use nanotopography to modify their surface to render it bioactive is particularly attractive. To this end, the usefulness of a variety of potential designs, including titania nanotube arrays loaded with antibiotics (Figure 10), has been recently discussed as a potential strategy to address localized infections [223].

3.4. Sensing

Nanostructured titania has been investigated to develop a variety of electrochemical sensors, especially as applied to biomarkers for early disease diagnosis. Volatile organic compounds (VOCs) can be useful biomarkers for the early detection of a variety of pathological states, and therefore chemoresistive breath sensors for their detection are investigated, often using semiconducting metal oxides. To this end, various forms of nanostructured titania can be used, such as nanoparticles, nanotube arrays, and nanosheets, as recently reviewed [224]. Zinc-doped titania nanoparticles have been also proposed to develop glutamate sensors, as glutamate is a common food additive but also a useful biomarker, since abnormal levels were linked to pathologies such as epilepsy, Alzheimer's and Parkinson's diseases, ischemia, and amyotrophic lateral sclerosis [225].

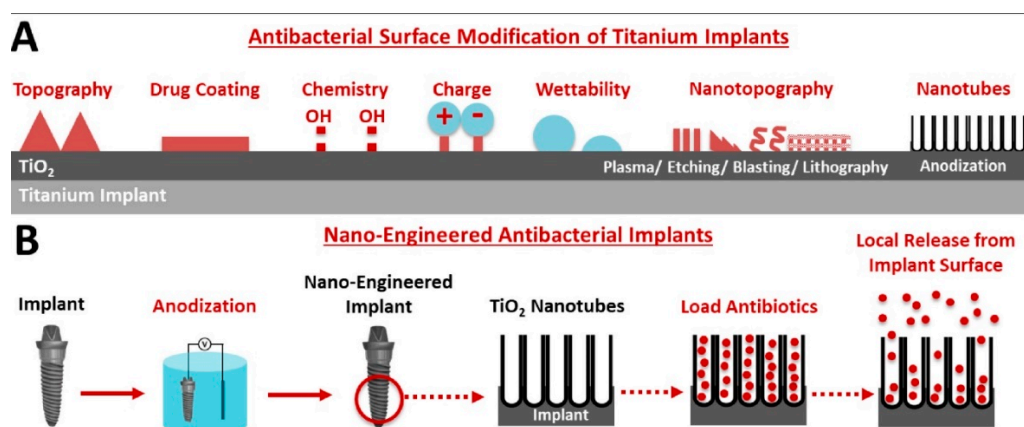


Figure 10. Schematic representation of (A) potential titanium–implant surface modification to attain antibacterial activity, and (B) in particular, the use of electrochemically anodized titania nanotube arrays for the local release of antibiotics. Reprinted from [223], Copyright © 2021, with permission from Elsevier.

For all these sensing applications, the inclusion of carbon nanostructures can be beneficial to enhance sensitivity and the performance of the devices generally, as recently reviewed [10]. This is true for a variety of carbon nanomorphologies. For instance, the inclusion of CNTs allowed a lower detection limit and an increased linear range of operativity for an epinephrine sensor [226]. In another recent example, an rGO/titania nanohybrid deposited on a glassy carbon electrode displayed a better performance for the electrochemical detection of a red dye relative to the sensor made with either component, thanks to a larger electroactive surface area and lower charge-transferred resistance [227]. Finally, graphene quantum dots also allowed for an enhanced photoresponse, with higher photocurrents and improved charge carrier separation efficiency, for an NO gas sensor based on titania that operated under UV-light irradiation [228].

4. Conclusions and Future Perspectives

The synergy between carbon nanostructures and titania has been extensively investigated over the years and allowed great progress in a variety of fields; in particular, for tailored applications to address urgent societal needs such as clean energy, medicine, and environmental remediation, which is now being extended to the issue of microplastics [229]. It has been undoubtedly demonstrated that the inclusion of nanocarbon into titania-based functional materials leads to the significant enhancement of the materials' properties. In photocatalysis, for example, depending on the efficiency of the titania/carbon contact, a clear reduction in the electron–hole recombination rate has been observed, as the nanocarbon scaffold is able to scavenge the photoexcited electrons. On the other hand, in electrocatalysis, the carbon conductivity has been exploited to facilitate the electron transfer processes occurring at the TiO₂-based catalytic sites, resulting in enhanced performances. Regardless of the application, it appears that the suitable interface between the carbon and the TiO₂ phases is in most cases an essential parameter to gain definite advantages in performance. For this reason, we have seen that efforts have focused on the development of synthetic protocols that could guarantee adequate phase contact, giving rise to the desired synergistic effects. As an example, the production of co-axial CNT–titania nanostructures, with an intimate contact between the two phases, could be attained through the careful selection of CNT functionalization, so that the support displays suitable oxygen-bearing functional groups to effectively anchor titania, and the optimization of the thermal annealing step to seal the CNT–titania interface [230].

The main limitation of titania for use in photochemical applications, namely its relatively wide bandgap that makes it unresponsive to visible light, has been linked in recent times to a predicted slow decline in the popularity of titania-based materials for photochemical sustainable processes, paving the way for the exploration of new semiconductor

materials with a more profitable exploitation of sunlight. However, we foresee that TiO₂ will still have a long life as the leading semiconductor as many authors have shown avenues for expanding its use to incorporate the exploitation of visible light. For example, defect engineering in TiO₂ polymorphs has reached a deep level of understanding, and the controlled alteration of the TiO₂ structure at atomic level can lead to considerable advantages. Black titania, obtained in 2011 by an intensive H₂ treatment that causes reduced Ti states by means of oxygen atom removal, is a symbolic case of a visible-light active TiO₂ material [231]. As the activity under visible light is caused by intragap states, it is frequently hypothesized that combined nanocarbon–TiO₂ could cause a C-doping of the titania at the phase interface, creating new midgap states.

TiO₂ is being revisited in modern times as a component in more complex composites, and the interfacing with carbon nanostructures certainly brings many advantages (some of them illustrated above), in concomitance with a confinement at the nanoscale level of the material, with the expected benefits of nanomaterials. However, TiO₂ junctions with other semiconductors bearing suitable electronic features could make further amends for the intrinsic shortcoming of self-standing TiO₂. Z-schemes or *p-n* heterojunctions are the two best known examples to improve photochemical properties. Therefore, opportune multi-phase nanohybrids or nanocomposites featuring nanocarbon and TiO₂ in conjunction with other components bear great potential for unlocking new multifunctionalities and directing these properties to specific purpose.

As we advance our detailed understanding of the mechanisms of interactions and reactions of nanostructured titania, further progress is set to be realized in this fascinating field. New opportunities are arising also from studies on surfaces [232]. The use of photoluminescence spectroscopy is emerging as a key tool to unravel mechanistic details of photocatalytic processes [233]. Finally, chiral nanostructures that can be attained through the templating of self-assembling molecules are also opening the door to new opportunities in non-linear optics, sensing, and photonics [234]. Examples of potential applications include circular polarizers, since titania chiral superstructures showed strong optical activity due to the difference of absorbing left and right-handed circularly polarized light [235]. Optically active films were also obtained from anatase nanocrystals that were spatially organized with long-range chiral nematic ordering, allowing for the selective reflection of circularly polarized light and iridescence [236].

Another emerging area of application lies in electronics and memory devices [114,237,238]. A recent report noted that the doping of titania with hydrogen, deuterium, and lithium led to bipolar conduction and a giant positive magnetoresistance, thus significantly expanding the properties of the materials [239]. Doping with cerium enhanced the magnetic properties of semiconductors from UV-light irradiation, thanks to the ferromagnetic orientation of spin densities near oxygen vacancies in Ce-doped titania, as opposed to the anti-ferromagnetic orientations of those found in undoped titania [240].

In conclusion, it appears that there is still a bright future ahead for the application of titania's great ability to interact with light, especially if maximized through the synergy with other nanomaterials and advanced techniques of characterization and fabrication.

Author Contributions: Writing—original draft preparation, M.C.C.; writing—review and editing, S.P., P.F. and S.M. All authors have read and agreed to the published version of the manuscript.

Funding: Part of the described research was funded by EU H2020 NMBP-SPIRE project, grant no. 820723, and by Italian Ministry of University and Research (MIUR) PRIN2015 project number 2015TWP83Z.

Acknowledgments: The authors would like to thank Antonella Orvati and Cristina Cocover for their valuable assistance with the library services. The authors would like to acknowledge COST Action EsSENce CA19118.

Conflicts of Interest: The authors declare no conflict of interest.

References

- Kumaravel, V.; Nair, K.M.; Mathew, S.; Bartlett, J.; Kennedy, J.E.; Manning, H.G.; Whelan, B.J.; Leyland, N.S.; Pillai, S.C. Antimicrobial TiO₂ nanocomposite coatings for surfaces, dental and orthopaedic implants. *Chem. Eng. J.* **2021**, *416*, 129071. [\[CrossRef\]](#) [\[PubMed\]](#)
- Dell'Edera, M.; Lo Porto, C.; De Pasquale, I.; Petronella, F.; Curri, M.L.; Agostiano, A.; Comparelli, R. Photocatalytic TiO₂-based coatings for environmental applications. *Catal. Today* **2021**. [\[CrossRef\]](#)
- Pereira Lopes, R.; Astruc, D. Biochar as a support for nanocatalysts and other reagents: Recent advances and applications. *Coord. Chem. Rev.* **2021**, *426*, 213585. [\[CrossRef\]](#)
- Piątkowska, A.; Janus, M.; Szymański, K.; Mozia, S. C-,N- and S-Doped TiO₂ Photocatalysts: A Review. *Catalysts* **2021**, *11*, 144. [\[CrossRef\]](#)
- Wang, S.; Ding, Z.; Chang, X.; Xu, J.; Wang, D.-H. Modified Nano-TiO₂ Based Composites for Environmental Photocatalytic Applications. *Catalysts* **2020**, *10*, 759. [\[CrossRef\]](#)
- Ijaz, M.; Zafar, M. Titanium dioxide nanostructures as efficient photocatalyst: Progress, challenges and perspective. *Int. J. Energy Res.* **2021**, *45*, 3569–3589. [\[CrossRef\]](#)
- Govardhana Reddy, P.V.; Rajendra Prasad Reddy, B.; Venkata Krishna Reddy, M.; Raghava Reddy, K.; Shetti, N.P.; Saleh, T.A.; Aminabhavi, T.M. A review on multicomponent reactions catalysed by zero-dimensional/one-dimensional titanium dioxide (TiO₂) nanomaterials: Promising green methodologies in organic chemistry. *J. Environ. Man.* **2021**, *279*, 111603. [\[CrossRef\]](#)
- Sudarsanam, P.; Li, H.; Sagar, T.V. TiO₂-Based Water-Tolerant Acid Catalysis for Biomass-Based Fuels and Chemicals. *ACS Catal.* **2020**, *10*, 9555–9584. [\[CrossRef\]](#)
- Huo, J.; Tessonnier, J.-P.; Shanks, B.H. Improving Hydrothermal Stability of Supported Metal Catalysts for Biomass Conversions: A Review. *ACS Catal.* **2021**, *11*, 5248–5270. [\[CrossRef\]](#)
- Nunes Simonetti, E.A.; Cardoso de Oliveira, T.; Enrico do Carmo Machado, Á.; Coutinho Silva, A.A.; Silva dos Santos, A.; de Simone Cividanes, L. TiO₂ as a gas sensor: The novel carbon structures and noble metals as new elements for enhancing sensitivity—A review. *Ceram. Int.* **2021**, *47*, 17844–17876. [\[CrossRef\]](#)
- Melchionna, M.; Prato, M.; Fornasiero, P. Mix and match metal oxides and nanocarbons for new photocatalytic frontiers. *Catal. Today* **2016**, *277*, 202–213. [\[CrossRef\]](#)
- Huang, J.-F.; Lei, Y.; Luo, T.; Liu, J.-M. Photocatalytic H₂ Production from Water by Metal-free Dye-sensitized TiO₂ Semiconductors: The Role and Development Process of Organic Sensitizers. *ChemSusChem* **2020**, *13*, 5863–5895. [\[CrossRef\]](#) [\[PubMed\]](#)
- Song, H.; Wei, L.; Chen, L.; Zhang, H.; Su, J. Photocatalytic Production of Hydrogen Peroxide over Modified Semiconductor Materials: A Minireview. *Top. Catal.* **2020**, *63*, 895–912. [\[CrossRef\]](#)
- Wu, W.-Q.; Feng, H.-L.; Chen, H.-Y.; Kuang, D.-B.; Su, C.-Y. Recent advances in hierarchical three-dimensional titanium dioxide nanotree arrays for high-performance solar cells. *J. Mater. Chem. A* **2017**, *5*, 12699–12717. [\[CrossRef\]](#)
- Žerjav, G.; Pintar, A. Influence of TiO₂ Morphology and Crystallinity on Visible-Light Photocatalytic Activity of TiO₂-Bi₂O₃ Composite in AOPs. *Catalysts* **2020**, *10*, 395. [\[CrossRef\]](#)
- Fischer, K.; Gawel, A.; Rosen, D.; Krause, M.; Abdul Latif, A.; Griebel, J.; Prager, A.; Schulze, A. Low-Temperature Synthesis of Anatase/Rutile/Brookite TiO₂ Nanoparticles on a Polymer Membrane for Photocatalysis. *Catalysts* **2017**, *7*, 209. [\[CrossRef\]](#)
- Sun, J.; Sun, J.; Wang, X. Anatase TiO₂ with Co-exposed (001) and (101) Surface-Based Photocatalytic Materials for Energy Conversion and Environmental Purification. *Chem. Asian J.* **2020**, *15*, 4168–4183. [\[CrossRef\]](#) [\[PubMed\]](#)
- Parashar, M.; Shukla, V.K.; Singh, R. Metal oxides nanoparticles via sol–gel method: A review on synthesis, characterization and applications. *J. Mater. Sci.* **2020**, *31*, 3729–3749. [\[CrossRef\]](#)
- Hidayat, R.; Fadillah, G.; Wahyuningsih, S. A control of TiO₂ nanostructures by hydrothermal condition and their application: A short review. *IOP Conf. Ser. Mater. Sci. Eng.* **2019**, *578*, 012031. [\[CrossRef\]](#)
- Mamaghani, A.H.; Haghighat, F.; Lee, C.-S. Hydrothermal/solvothermal synthesis and treatment of TiO₂ for photocatalytic degradation of air pollutants: Preparation, characterization, properties, and performance. *Chemosphere* **2019**, *219*, 804–825. [\[CrossRef\]](#) [\[PubMed\]](#)
- Pimentel, A.; Nunes, D.; Pereira, S.; Martins, R.; Fortunato, E. Photocatalytic Activity of TiO₂ nanostructured arrays prepared by microwave-assisted solvothermal method. In *Semiconductor Photocatalysis: Materials, Mechanisms and Applications*; Cao, W., Ed.; IntechOpen: London, UK, 2016; pp. 81–103.
- Nie, X.; Yin, S.; Duan, W.; Zhao, Z.; Li, L.; Zhang, Z. Recent Progress in Anodic Oxidation of TiO₂ Nanotubes and Enhanced Photocatalytic Performance: A Short Review. *Nano* **2021**, *16*, 2130002. [\[CrossRef\]](#)
- Niemelä, J.-P.; Marin, G.; Karppinen, M. Titanium dioxide thin films by atomic layer deposition: A review. *Semicond. Sci. Tech.* **2017**, *32*, 093005. [\[CrossRef\]](#)
- Siuzdak, K.; Haryński, Ł.; Wawrzyniak, J.; Grochowska, K. Review on robust laser light interaction with titania—Patterning, crystallisation and ablation processes. *Prog. Solid State Chem.* **2021**, *62*, 100297. [\[CrossRef\]](#)
- Jayanthi, S.; Sarkar, D.; Taffa, D.H.; Yerushalmi, R. Photoreactivity of Deep VB Titania Attained Via Molecular Layer Deposition; Interplay of Metal Oxide Thin Film Built-in Strain and Molecular Effects. *Top. Catal.* **2021**, *64*, 297–312. [\[CrossRef\]](#)
- Thalib Basha, G.M.; Srikanth, A.; Venkateshwarlu, B. A Critical Review on Nano structured Coatings for Alumina-Titania (Al₂O₃-TiO₂) Deposited by Air Plasma Spraying Process (APS). *Mater. Today Proc.* **2020**, *22*, 1554–1562. [\[CrossRef\]](#)

27. Georgakilas, V.; Perman, J.A.; Tucek, J.; Zboril, R. Broad family of carbon nanoallotropes: Classification, chemistry, and applications of fullerenes, carbon dots, nanotubes, graphene, nanodiamonds, and combined superstructures. *Chem. Rev.* **2015**, *115*, 4744–4822. [\[CrossRef\]](#)
28. Basso, L.; Cazzanelli, M.; Orlandi, M.; Miotello, A. Nanodiamonds: Synthesis and application in sensing, catalysis, and the possible connection with some processes occurring in space. *Appl. Sci.* **2020**, *10*, 4094. [\[CrossRef\]](#)
29. Wang, Y.; Yang, P.; Zheng, L.; Shi, X.; Zheng, H. Carbon nanomaterials with sp² or/and sp hybridization in energy conversion and storage applications: A review. *Energy Storage Mater.* **2020**, *26*, 349–370. [\[CrossRef\]](#)
30. Bryce, M.R. A review of functional linear carbon chains (oligoynes, polyynes, cumulenes) and their applications as molecular wires in molecular electronics and optoelectronics. *J. Mater. Chem. C* **2021**. [\[CrossRef\]](#)
31. Adorinni, S.; Cringoli, M.C.; Perathoner, S.; Fornasiero, P.; Marchesan, S. Green Approaches to Carbon Nanostructure-Based Biomaterials. *Appl. Sci.* **2021**, *11*, 2490. [\[CrossRef\]](#)
32. Ugarte, D. Onion-like graphitic particles. In *Carbon Nanotubes*; Elsevier: Amsterdam, The Netherlands, 1996; pp. 163–167.
33. Zieleniewska, A.; Lodermeier, F.; Roth, A.; Guldi, D.M. Fullerenes—how 25 years of charge transfer chemistry have shaped our understanding of (interfacial) interactions. *Chem. Soc. Rev.* **2018**, *47*, 702–714. [\[CrossRef\]](#) [\[PubMed\]](#)
34. Yang, F.; Wang, M.; Zhang, D.; Yang, J.; Zheng, M.; Li, Y. Chirality pure carbon nanotubes: Growth, sorting, and characterization. *Chem. Rev.* **2020**, *120*, 2693–2758. [\[CrossRef\]](#)
35. Bottari, G.; Herranz, M.Á.; Wibmer, L.; Volland, M.; Rodríguez-Pérez, L.; Guldi, D.M.; Hirsch, A.; Martín, N.; D’Souza, F.; Torres, T. Chemical functionalization and characterization of graphene-based materials. *Chem. Soc. Rev.* **2017**, *46*, 4464–4500. [\[CrossRef\]](#)
36. Dhand, V.; Yadav, M.; Kim, S.H.; Rhee, K.Y. A comprehensive review on the prospects of multi-functional carbon nano onions as an effective, high-performance energy storage material. *Carbon* **2021**, *175*, 534–575. [\[CrossRef\]](#)
37. Karousis, N.; Suarez-Martinez, I.; Ewels, C.P.; Tagmatarchis, N. Structure, properties, functionalization, and applications of carbon nanohorns. *Chem. Rev.* **2016**, *116*, 4850–4883. [\[CrossRef\]](#)
38. Stepanidenko, E.A.; Ushakova, E.V.; Fedorov, A.V.; Rogach, A.L. Applications of Carbon Dots in Optoelectronics. *Nanomaterials* **2021**, *11*, 364. [\[CrossRef\]](#)
39. Marchesan, S.; Melchionna, M.; Prato, M. Wire Up on Carbon Nanostructures! How To Play a Winning Game. *ACS Nano* **2015**, *9*, 9441–9450. [\[CrossRef\]](#)
40. Shi, C.; Owusu, K.A.; Xu, X.; Zhu, T.; Zhang, G.; Yang, W.; Mai, L. 1D Carbon-Based Nanocomposites for Electrochemical Energy Storage. *Small* **2019**, *15*, 1902348. [\[CrossRef\]](#) [\[PubMed\]](#)
41. Hu, C.; Qu, J.; Xiao, Y.; Zhao, S.; Chen, H.; Dai, L. Carbon Nanomaterials for Energy and Biorelated Catalysis: Recent Advances and Looking Forward. *ACS Cent. Sci.* **2019**, *5*, 389–408. [\[CrossRef\]](#)
42. Ortiz-Medina, J.; Wang, Z.; Cruz-Silva, R.; Morelos-Gomez, A.; Wang, F.; Yao, X.; Terrones, M.; Endo, M. Defect Engineering and Surface Functionalization of Nanocarbons for Metal-Free Catalysis. *Adv. Mater.* **2019**, *31*, 1805717. [\[CrossRef\]](#)
43. Zhang, L.; Lin, C.-Y.; Zhang, D.; Gong, L.; Zhu, Y.; Zhao, Z.; Xu, Q.; Li, H.; Xia, Z. Guiding Principles for Designing Highly Efficient Metal-Free Carbon Catalysts. *Adv. Mater.* **2019**, *31*, 1805252. [\[CrossRef\]](#)
44. Hu, C.; Dai, L. Doping of Carbon Materials for Metal-Free Electrocatalysis. *Adv. Mater.* **2019**, *31*, 180467. [\[CrossRef\]](#)
45. Sideri, I.K.; Tagmatarchis, N. Noble-Metal-Free Doped Carbon Nanomaterial Electrocatalysts. *Chem. Eur. J.* **2020**, *26*, 15397–15415. [\[CrossRef\]](#)
46. Ding, H.; Hu, B.; Zhang, B.; Zhang, H.; Yan, X.; Nie, G.; Liang, M. Carbon-based nanozymes for biomedical applications. *Nano Res.* **2021**, *14*, 570–583. [\[CrossRef\]](#)
47. Park, S.-J.; Deshmukh, M.A.; Kang, B.-C.; Jeon, J.-Y.; Chen, C.; Ha, T.-J. Review—A Review of Advanced Electronic Applications Based on Carbon Nanomaterials. *ECS J. Solid State Sci. Technol.* **2020**, *9*, 071002. [\[CrossRef\]](#)
48. Benzigar, M.R.; Dasireddy, V.D.B.C.; Guan, X.; Wu, T.; Liu, G. Advances on Emerging Materials for Flexible Supercapacitors: Current Trends and Beyond. *Adv. Funct. Mater.* **2020**, *30*, 2002993. [\[CrossRef\]](#)
49. Iglesias, D.; Senokos, E.; Alemán, B.; Cabana, L.; Navío, C.; Marcilla, R.; Prato, M.; Vilatela, J.J.; Marchesan, S. Gas-Phase Functionalization of Macroscopic Carbon Nanotube Fiber Assemblies: Reaction Control, Electrochemical Properties, and Use for Flexible Supercapacitors. *ACS Appl. Mater. Interfaces* **2018**, *10*, 5760–5770. [\[CrossRef\]](#) [\[PubMed\]](#)
50. Chen, S.; Kuang, Q.; Fan, H.J. Dual-Carbon Batteries: Materials and Mechanism. *Small* **2020**, *16*, 2002803. [\[CrossRef\]](#) [\[PubMed\]](#)
51. Wu, Z.; Wang, Y.; Liu, X.; Lv, C.; Li, Y.; Wei, D.; Liu, Z. Carbon-Nanomaterial-Based Flexible Batteries for Wearable Electronics. *Adv. Mater.* **2019**, *31*, 1800716. [\[CrossRef\]](#) [\[PubMed\]](#)
52. Khalid, M.; Bhardwaj, P.A.; Honorato, A.M.B.; Varela, H. Metallic single-atoms confined in carbon nanomaterials for the electrocatalysis of oxygen reduction, oxygen evolution, and hydrogen evolution reactions. *Catal. Sci. Technol.* **2020**, *10*, 6420–6448. [\[CrossRef\]](#)
53. Gupta, S.; Tai, N.-H. Carbon materials and their composites for electromagnetic interference shielding effectiveness in X-band. *Carbon* **2019**, *152*, 159–187. [\[CrossRef\]](#)
54. Zhang, J.; Deng, Y.; Hu, X.; Chi, X.; Liu, J.; Chu, W.; Sun, L. Molecular Magnets Based on Graphenes and Carbon Nanotubes. *Adv. Mater.* **2019**, *31*, 1804917. [\[CrossRef\]](#)
55. Zhang, G.; Koman, V.B.; Shikdar, T.; Oliver, R.J.; Perez-Lodeiro, N.; Strano, M.S. High Thermal Effusivity Nanocarbon Materials for Resonant Thermal Energy Harvesting. *Small* **2021**, 2006752. [\[CrossRef\]](#)

56. Howlader, A.H.; Li, F.; Zheng, R. Carbon Nanomaterials for Halide Perovskites-Based Hybrid Photodetectors. *Adv. Mater. Technol.* **2020**, *5*, 2000643. [\[CrossRef\]](#)
57. Asadian, E.; Ghalkhani, M.; Shahrokhian, S. Electrochemical sensing based on carbon nanoparticles: A review. *Sensor. Actuat. B Chem.* **2019**, *293*, 183–209. [\[CrossRef\]](#)
58. Speranza, G. Carbon Nanomaterials: Synthesis, Functionalization and Sensing Applications. *Nanomaterials* **2021**, *11*, 967. [\[CrossRef\]](#) [\[PubMed\]](#)
59. Shi, J.-X.; Lei, X.-W.; Natsuki, T. Review on Carbon Nanomaterials-Based Nano-Mass and Nano-Force Sensors by Theoretical Analysis of Vibration Behavior. *Sensors* **2021**, *21*, 1907. [\[CrossRef\]](#)
60. Bag, A.; Lee, N.-E. Recent Advancements in Development of Wearable Gas Sensors. *Adv. Mater. Technol.* **2021**, *6*, 2000883. [\[CrossRef\]](#)
61. Joshi, P.; Mishra, R.; Narayan, R.J. Biosensing applications of carbon-based materials. *Curr. Opin. Biomed. Eng.* **2021**, *18*, 100274. [\[CrossRef\]](#)
62. Chen, Z.; Zhao, D.; Ma, R.; Zhang, X.; Rao, J.; Yin, Y.; Wang, X.; Yi, F. Flexible temperature sensors based on carbon nanomaterials. *J. Mater. Chem. B* **2021**, *9*, 1941–1964. [\[CrossRef\]](#)
63. Biswas, S.; Visell, Y. Emerging Material Technologies for Haptics. *Adv. Mater. Technol.* **2019**, *4*, 1900042. [\[CrossRef\]](#)
64. Thamaraiselvan, C.; Wang, J.; James, D.K.; Narkhede, P.; Singh, S.P.; Jassby, D.; Tour, J.M.; Arnusch, C.J. Laser-induced graphene and carbon nanotubes as conductive carbon-based materials in environmental technology. *Mater. Today* **2020**, *34*, 115–131. [\[CrossRef\]](#)
65. Gusain, R.; Kumar, N.; Ray, S.S. Recent advances in carbon nanomaterial-based adsorbents for water purification. *Coord. Chem. Rev.* **2020**, *405*, 213111. [\[CrossRef\]](#)
66. Su, D.; Li, H.; Yan, X.; Lin, Y.; Lu, G. Biosensors based on fluorescence carbon nanomaterials for detection of pesticides. *Trends Anal. Chem.* **2021**, *134*, 116126. [\[CrossRef\]](#)
67. Torrinha, Á.; Oliveira, T.M.B.F.; Ribeiro, F.W.P.; Correia, A.N.; Lima-Neto, P.; Morais, S. Application of Nanostructured Carbon-Based Electrochemical (Bio)Sensors for Screening of Emerging Pharmaceutical Pollutants in Waters and Aquatic Species: A Review. *Nanomaterials* **2020**, *10*, 1268. [\[CrossRef\]](#)
68. Wang, G.; Liu, L.; Zhang, Z. Interface mechanics in carbon nanomaterials-based nanocomposites. *Compos. Part A Appl. Sci. Manuf.* **2021**, *141*, 106212. [\[CrossRef\]](#)
69. Iglesias, D.; Bosi, S.; Melchionna, M.; Da Ros, T.; Marchesan, S. The glitter of carbon nanostructures in hybrid/composite hydrogels for medicinal use. *Curr. Top. Med. Chem.* **2016**, *16*, 1976–1989. [\[CrossRef\]](#) [\[PubMed\]](#)
70. Araby, S.; Philips, B.; Meng, Q.; Ma, J.; Laoui, T.; Wang, C.H. Recent advances in carbon-based nanomaterials for flame retardant polymers and composites. *Compos. Part B Eng.* **2021**, *212*, 108675. [\[CrossRef\]](#)
71. Marchesan, S.; Melchionna, M.; Prato, M. Carbon Nanostructures for Nanomedicine: Opportunities and Challenges. *Fuller. Nanotub. Carbon Nanostruct.* **2014**, *22*, 190–195. [\[CrossRef\]](#)
72. Riley, P.R.; Narayan, R.J. Recent advances in carbon nanomaterials for biomedical applications: A review. *Curr. Opin. Biomed. Eng.* **2021**, *17*, 100262. [\[CrossRef\]](#)
73. Plachá, D.; Jampilek, J. Graphenic Materials for Biomedical Applications. *Nanomaterials* **2019**, *9*, 1758. [\[CrossRef\]](#)
74. Loh, K.P.; Ho, D.; Chiu, G.N.C.; Leong, D.T.; Pastorin, G.; Chow, E.K. Clinical Applications of Carbon Nanomaterials in Diagnostics and Therapy. *Adv. Mater.* **2018**, *30*, e1802368. [\[CrossRef\]](#)
75. Mehra, N.K.; Jain, A.K.; Nahar, M. Carbon nanomaterials in oncology: An expanding horizon. *Drug Discov. Today* **2018**, *23*, 1016–1025. [\[CrossRef\]](#) [\[PubMed\]](#)
76. Jiang, B.-P.; Zhou, B.; Lin, Z.; Liang, H.; Shen, X.-C. Recent Advances in Carbon Nanomaterials for Cancer Phototherapy. *Chem. Eur. J.* **2019**, *25*, 3993–4004. [\[CrossRef\]](#) [\[PubMed\]](#)
77. Patel, K.D.; Singh, R.K.; Kim, H.-W. Carbon-based nanomaterials as an emerging platform for theranostics. *Mater. Horiz.* **2019**, *6*, 434–469. [\[CrossRef\]](#)
78. Jampilek, J.; Kralova, K. Advances in Drug Delivery Nanosystems Using Graphene-Based Materials and Carbon Nanotubes. *Materials* **2021**, *14*, 1059. [\[CrossRef\]](#) [\[PubMed\]](#)
79. Xin, Q.; Shah, H.; Nawaz, A.; Xie, W.; Akram, M.Z.; Batool, A.; Tian, L.; Jan, S.U.; Boddula, R.; Guo, B. Antibacterial carbon-based nanomaterials. *Adv. Mater.* **2019**, *31*, 1804838. [\[CrossRef\]](#)
80. Innocenzi, P.; Stagi, L. Carbon-based antiviral nanomaterials: Graphene, C-dots, and fullerenes. A perspective. *Chem. Sci.* **2020**, *11*, 6606–6622. [\[CrossRef\]](#)
81. Rasheed, P.A.; Sandhyarani, N. Carbon nanostructures as immobilization platform for DNA: A review on current progress in electrochemical DNA sensors. *Biosens. Bioelectron.* **2017**, *97*, 226–237. [\[CrossRef\]](#)
82. Ku, S.H.; Lee, M.; Park, C.B. Carbon-based nanomaterials for tissue engineering. *Adv. Healthc. Mater.* **2013**, *2*, 244–260. [\[CrossRef\]](#)
83. Marchesan, S.; Ballerini, L.; Prato, M. Nanomaterials for stimulating nerve growth. *Science* **2017**, *356*, 1010–1011. [\[CrossRef\]](#)
84. Marchesan, S.; Bosi, S.; Alshatwi, A.; Prato, M. Carbon nanotubes for organ regeneration: An electrifying performance. *Nano Today* **2016**, *11*, 398–401. [\[CrossRef\]](#)
85. Peng, Z.; Zhao, T.; Zhou, Y.; Li, S.; Li, J.; Leblanc, R.M. Bone Tissue Engineering via Carbon-Based Nanomaterials. *Adv. Healthc. Mater.* **2020**, *9*, 1901495. [\[CrossRef\]](#) [\[PubMed\]](#)

86. Du, C.; Ren, Y.; Qu, Z.; Gao, L.; Zhai, Y.; Han, S.-T.; Zhou, Y. Synaptic transistors and neuromorphic systems based on carbon nano-materials. *Nanoscale* **2021**, *13*, 7498–7522. [[CrossRef](#)] [[PubMed](#)]
87. Lee, K.; Yoon, H.; Ahn, C.; Park, J.; Jeon, S. Strategies to improve the photocatalytic activity of TiO₂: 3D nanostructuring and heterostructuring with graphitic carbon nanomaterials. *Nanoscale* **2019**, *11*, 7025–7040. [[CrossRef](#)] [[PubMed](#)]
88. Melchionna, M.; Marchesan, S.; Fornasiero, P.; Prato, M. Carbon nanotubes and catalysis: The many facets of a successful marriage. *Catal. Sci. Technol.* **2015**, *5*, 3859–3875. [[CrossRef](#)]
89. Saha, A.; Moya, A.; Kahnt, A.; Iglesias, D.; Marchesan, S.; Wannemacher, R.; Prato, M.; Vilatela, J.J.; Guldi, D.M. Interfacial charge transfer in functionalized multi-walled carbon nanotube@TiO₂ nanofibres. *Nanoscale* **2017**, *9*, 7911–7921. [[CrossRef](#)]
90. Hamandi, M.; Meksi, M.; Kochkar, H. Nanoscale Advances of Carbon-Titanium Dioxide Nanomaterials in Photocatalysis Applications. *Rev. Nanosci. Nanotechnol.* **2016**, *4*, 108–134. [[CrossRef](#)]
91. Wang, Q.; Cai, J.; Biesold-McGee, G.V.; Huang, J.; Ng, Y.H.; Sun, H.; Wang, J.; Lai, Y.; Lin, Z. Silk fibroin-derived nitrogen-doped carbon quantum dots anchored on TiO₂ nanotube arrays for heterogeneous photocatalytic degradation and water splitting. *Nano Energy* **2020**, *78*, 105313. [[CrossRef](#)]
92. He, C.; Peng, L.; Lv, L.; Cao, Y.; Tu, J.; Huang, W.; Zhang, K. In situ growth of carbon dots on TiO₂ nanotube arrays for PEC enzyme biosensors with visible light response. *RSC Adv.* **2019**, *9*, 15084–15091. [[CrossRef](#)]
93. Huo, P.; Shi, X.; Zhang, W.; Kumar, P.; Liu, B. An overview on the incorporation of graphene quantum dots on TiO₂ for enhanced performances. *J. Mater. Sci.* **2021**, *56*, 6031–6051. [[CrossRef](#)]
94. Justh, N.; Firkala, T.; László, K.; Lábár, J.; Szilágyi, I.M. Photocatalytic C₆₀-amorphous TiO₂ composites prepared by atomic layer deposition. *Appl. Surf. Sci.* **2017**, *419*, 497–502. [[CrossRef](#)]
95. Zhang, Y.; Zhang, W.; Yang, K.; Yang, Y.; Jia, J.; Liang, Y.; Guo, L. Carbon Nano-Onions (CNOs)/TiO₂ Composite Preparation and Its Photocatalytic Performance under Visible Light Irradiation. *J. Environ. Eng.* **2020**, *146*, 04020009. [[CrossRef](#)]
96. Lim, E.; Shim, H.; Fleischmann, S.; Presser, V. Fast and stable lithium-ion storage kinetics of anatase titanium dioxide/carbon onion hybrid electrodes. *J. Mater. Chem. A* **2018**, *6*, 9480–9488. [[CrossRef](#)]
97. Mohapatra, D.; Parida, S.; Singh, B.K.; Sutar, D.S. Importance of microstructure and interface in designing metal oxide nanocomposites for supercapacitor electrodes. *J. Electroanal. Chem.* **2017**, *803*, 30–39. [[CrossRef](#)]
98. Melchionna, M.; Beltram, A.; Montini, T.; Monai, M.; Nasi, L.; Fornasiero, P.; Prato, M. Highly efficient hydrogen production through ethanol photoreforming by a carbon nanocone/Pd@TiO₂ hybrid catalyst. *Chem. Commun.* **2016**, *52*, 764–767. [[CrossRef](#)] [[PubMed](#)]
99. Melchionna, M.; Bracamonte, M.V.; Giuliani, A.; Nasi, L.; Montini, T.; Tavagnacco, C.; Bonchio, M.; Fornasiero, P.; Prato, M. Pd@TiO₂/carbon nanohorn electrocatalysts: Reversible CO₂ hydrogenation to formic acid. *Energy Environ. Sci.* **2018**, *11*, 1571–1580. [[CrossRef](#)]
100. Ramesh Reddy, N.; Mamatha Kumari, M.; Shankar, M.V.; Raghava Reddy, K.; Woo Joo, S.; Aminabhavi, T.M. Photocatalytic hydrogen production from dye contaminated water and electrochemical supercapacitors using carbon nanohorns and TiO₂ nanoflower heterogeneous catalysts. *J. Environ. Man.* **2021**, *277*, 111433. [[CrossRef](#)]
101. Piovesana, S.; Iglesias, D.; Melle-Franco, M.; Kralj, S.; Cavaliere, C.; Melchionna, M.; Laganà, A.; Capriotti, A.L.; Marchesan, S. Carbon nanostructure morphology templates nanocomposites for phosphoproteomics. *Nano Res.* **2020**, *13*, 380–388. [[CrossRef](#)]
102. Hunge, Y.M.; Yadav, A.A.; Khan, S.; Takagi, K.; Suzuki, N.; Teshima, K.; Terashima, C.; Fujishima, A. Photocatalytic degradation of bisphenol A using titanium dioxide@nanodiamond composites under UV light illumination. *J. Colloid Interf. Sci.* **2021**, *582*, 1058–1066. [[CrossRef](#)] [[PubMed](#)]
103. Henych, J.; Stehlík, Š.; Mazanec, K.; Tolasz, J.; Čermák, J.; Rezek, B.; Mattsson, A.; Österlund, L. Reactive adsorption and photodegradation of soman and dimethyl methylphosphonate on TiO₂/nanodiamond composites. *Appl. Catal. B Environ.* **2019**, *259*, 118097. [[CrossRef](#)]
104. Pastrana-Martínez, L.M.; Morales-Torres, S.; Carabineiro, S.A.C.; Buijnsters, J.G.; Figueiredo, J.L.; Silva, A.M.T.; Faria, J.L. Photocatalytic activity of functionalized nanodiamond-TiO₂ composites towards water pollutants degradation under UV/Vis irradiation. *Appl. Surf. Sci.* **2018**, *458*, 839–848. [[CrossRef](#)]
105. Gao, X.; Sun, X.; Jiang, Z.; Wang, Q.; Gao, N.; Li, H.; Zhang, H.; Yu, K.; Su, C. Introducing nanodiamond into TiO₂-based anode for improving the performance of lithium-ion batteries. *New J. Chem.* **2019**, *43*, 3907–3912. [[CrossRef](#)]
106. Park, H.-A.; Liu, S.; Salvador, P.A.; Rohrer, G.S.; Islam, M.F. High visible-light photochemical activity of titania decorated on single-wall carbon nanotube aerogels. *RSC Adv.* **2016**, *6*, 22285–22294. [[CrossRef](#)]
107. Kurniawan, K.; Tajima, T.; Kubo, Y.; Miyake, H.; Kurashige, W.; Negishi, Y.; Takaguchi, Y. Incorporating a TiO_x shell in single-walled carbon nanotube/fullerodendron coaxial nanowires: Increasing the photocatalytic evolution of H₂ from water under irradiation with visible light. *RSC Adv.* **2017**, *7*, 31767–31770. [[CrossRef](#)]
108. Acauan, L.; Dias, A.C.; Pereira, M.B.; Horowitz, F.; Bergmann, C.P. Influence of Different Defects in Vertically Aligned Carbon Nanotubes on TiO₂ Nanoparticle Formation through Atomic Layer Deposition. *ACS Appl. Mater. Interfaces* **2016**, *8*, 16444–16450. [[CrossRef](#)]
109. Delekar, S.D.; Dhodamani, A.G.; More, K.V.; Dongale, T.D.; Kamat, R.K.; Acquah, S.F.A.; Dalal, N.S.; Panda, D.K. Structural and Optical Properties of Nanocrystalline TiO₂ with Multiwalled Carbon Nanotubes and Its Photovoltaic Studies Using Ru(II) Sensitizers. *ACS Omega* **2018**, *3*, 2743–2756. [[CrossRef](#)] [[PubMed](#)]

110. Yang, H.M.; Park, S.-J. Effect of incorporation of multiwalled carbon nanotubes on photodegradation efficiency of mesoporous anatase TiO₂ spheres. *Mater. Chem. Phys.* **2017**, *186*, 261–270. [\[CrossRef\]](#)
111. Wan, L.; Deng, C.; Zhao, Z.-Y.; Zhao, H.-B.; Wang, Y.-Z. A titanium dioxide–carbon nanotube hybrid to simultaneously achieve the mechanical enhancement of natural rubber and its stability under extreme frictional conditions. *Mater. Adv.* **2021**, *2*, 2408–2418. [\[CrossRef\]](#)
112. Huang, M.; Chu, Y.; Xi, B.; Shi, N.; Duan, B.; Zhang, C.; Chen, W.; Feng, J.; Xiong, S. TiO₂-Based Heterostructures with Different Mechanism: A General Synergistic Effect toward High-Performance Sodium Storage. *Small* **2020**, *16*, 2004054. [\[CrossRef\]](#)
113. Sharma, H.K.; Sharma, S.K.; Vemula, K.; Koirala, A.R.; Yadav, H.M.; Singh, B.P. CNT facilitated interfacial charge transfer of TiO₂ nanocomposite for controlling the electron-hole recombination. *Solid State Sci.* **2021**, *112*, 106492. [\[CrossRef\]](#)
114. Mohamed, H.H.; Mohamed, S.K. Rutile TiO₂ nanorods/MWCNT composites for enhanced simultaneous photocatalytic oxidation of organic dyes and reduction of metal ions. *Mater. Res. Express* **2018**, *5*, 015057. [\[CrossRef\]](#)
115. Mullani, N.; Ali, I.; Dongale, T.D.; Kim, G.H.; Choi, B.J.; Basit, M.A.; Park, T.J. Improved resistive switching behavior of multiwalled carbon nanotube/TiO₂ nanorods composite film by increased oxygen vacancy reservoir. *Mater. Sci. Semicond. Proc.* **2020**, *108*, 104907. [\[CrossRef\]](#)
116. Yang, J.; Cheng, J.; Tao, J.; Higashi, M.; Yamauchi, M.; Nakashima, N. Wrapping Multiwalled Carbon Nanotubes with Anatase Titanium Oxide for the Electrosynthesis of Glycolic Acid. *ACS Appl. Nano Mater.* **2019**, *2*, 6360–6367. [\[CrossRef\]](#)
117. Ghosh, S.; Kiran Kumar, V.; Kumar, S.K.; Biswas, S.; Martha, S.K. An insight of sodium-ion storage, diffusivity into TiO₂ nanoparticles and practical realization to sodium-ion full cell. *Electrochim. Acta* **2019**, *316*, 69–78. [\[CrossRef\]](#)
118. Song, L.; Chen, P.; Li, Z.; Du, P.; Yang, Y.; Li, N.; Xiong, J. Flexible carbon nanotubes/TiO₂/C nanofibrous film as counter electrode of flexible quasi-solid dye-sensitized solar cells. *Thin Solid Film.* **2020**, *711*, 138307. [\[CrossRef\]](#)
119. Zhu, K.; Li, C.; Jiao, Y.; Zhu, J.; Ren, H.; Luo, Y.; Fan, S.; Liu, K. Free-standing hybrid films comprising of ultra-dispersed titania nanocrystals and hierarchical conductive network for excellent high rate performance of lithium storage. *Nano Res.* **2020**. [\[CrossRef\]](#)
120. Zou, M.; Ma, Z.; Wang, Q.; Yang, Y.; Wu, S.; Yang, L.; Hu, S.; Xu, W.; Han, P.; Zou, R.; et al. Coaxial TiO₂–carbon nanotube sponges as compressible anodes for lithium-ion batteries. *J. Mater. Chem. A* **2016**, *4*, 7398–7405. [\[CrossRef\]](#)
121. Beltram, A.; Melchionna, M.; Montini, T.; Nasi, L.; Fornasiero, P.; Prato, M. Making H₂ from light and biomass-derived alcohols: The outstanding activity of newly designed hierarchical MWCNT/Pd@TiO₂ hybrid catalysts. *Green Chem.* **2017**, *19*, 2379–2389. [\[CrossRef\]](#)
122. Mo, Z.; Yang, R.; Lu, D.; Yang, L.; Hu, Q.; Li, H.; Zhu, H.; Tang, Z.; Gui, X. Lightweight, three-dimensional carbon Nanotube@TiO₂ sponge with enhanced microwave absorption performance. *Carbon* **2019**, *144*, 433–439. [\[CrossRef\]](#)
123. Belkhanchi, H.; Ziat, Y.; Hammi, M.; Laghlimi, C.; Moutcine, A.; Benyounes, A.; Kzaiber, F. Nitrogen doped carbon nanotubes grafted TiO₂ rutile nanofilms: Promising material for dye sensitized solar cell application. *Optik* **2021**, *229*, 166234. [\[CrossRef\]](#)
124. Wang, Q.; Wang, Y.; Duan, B.; Zhang, M. Modified Sol-Gel Synthesis of Carbon Nanotubes Supported Titania Composites with Enhanced Visible Light Induced Photocatalytic Activity. *J. Nanomater.* **2016**, *2016*, 3967156. [\[CrossRef\]](#)
125. Samadi, A.; Ahmadi, R.; Hosseini, S.M. Influence of TiO₂-Fe₃O₄-MWCNT hybrid nanotubes on piezoelectric and electromagnetic wave absorption properties of electrospun PVDF nanocomposites. *Org. Electron.* **2019**, *75*, 105405. [\[CrossRef\]](#)
126. Lu, X.; Luo, F.; Tian, Q.; Zhang, W.; Sui, Z.; Chen, J. Anatase TiO₂ nanowires intertwined with CNT for conductive additive-free lithium-ion battery anodes. *J. Phys. Chem. Solids* **2021**, *153*, 110037. [\[CrossRef\]](#)
127. Akram, M.; Khan, R.M.; Afzal, F.; Mustafa, G.M.; Ahmad, A.; Ramay, S.M.; Mahmood, A.; Ali, S.M.; Atiq, S. CNTs mediated electrochemical performance and dielectric dispersion of TiO₂-based hydrothermally synthesized nanocomposites. *Ionics* **2021**, *27*, 2107–2118. [\[CrossRef\]](#)
128. Vajda, K.; Hernádi, K.; Coteș, C.; Kovács, G.; Pap, Z. Shape-Tailored TiO₂ Photocatalysts Obtained in the Presence of Different Types of Carbon Materials. *J. Nanosci. Nanotechnol.* **2021**, *21*, 2360–2367. [\[CrossRef\]](#)
129. Idris, N.J.; Bakar, S.A.; Mohamed, A.; Muqoyyanah, M.; Othman, M.H.D.; Mamat, M.H.; Ahmad, M.K.; Birowosuto, M.D.; Soga, T. Photocatalytic performance improvement by utilizing GO_MWCNTs hybrid solution on sand/ZnO/TiO₂-based photocatalysts to degrade methylene blue dye. *Environ. Sci. Pollut. Res.* **2021**, *28*, 6966–6979. [\[CrossRef\]](#)
130. Zhao, S.; Ding, H.; Chen, J.; Yang, C.; Xian, X. Facile synthesis of CNTs@TiO₂ composites by solvothermal reaction for high-rate and long-life lithium-ion batteries. *J. Phys. Chem. Solids* **2021**, *152*, 109950. [\[CrossRef\]](#)
131. Jiang, K.; Niu, Y.; Fang, D.; Zhang, L.; Wang, C. Sulfur Incorporation in Hierarchical TiO₂ Nanosheet/Carbon Nanotube Hybrids for Improved Lithium Storage Performance. *ChemElectroChem* **2020**, *7*, 2905–2916. [\[CrossRef\]](#)
132. Silva, M.R.F.; Lourenço, M.A.O.; Tobaldi, D.M.; da Silva, C.F.; Seabra, M.P.; Ferreira, P. Carbon-modified titanium oxide materials for photocatalytic water and air decontamination. *Chem. Eng. J.* **2020**, *387*, 124099. [\[CrossRef\]](#)
133. Zhu, C.; Tang, Y.; Liu, L.; Sheng, R.; Li, X.; Gao, Y.; NuLi, Y. A high-performance rechargeable Mg²⁺/Li⁺ hybrid battery using CNT@TiO₂ nanocables as the cathode. *J. Colloid Interf. Sci.* **2021**, *581*, 307–313. [\[CrossRef\]](#)
134. Liang, Z.; Bai, X.; Hao, P.; Guo, Y.; Xue, Y.; Tian, J.; Cui, H. Full solar spectrum photocatalytic oxygen evolution by carbon-coated TiO₂ hierarchical nanotubes. *Appl. Catal. B Environ.* **2019**, *243*, 711–720. [\[CrossRef\]](#)
135. Xia, Y.; Xiong, W.-S.; Jiang, Y.; Sun, W.; Sang, H.-Q.; He, R.-X.; Tai, Q.; Chen, B.; Liu, Y.; Zhao, X.-Z. Multi-walled carbon nanotubes induced a controllable TiO₂ morphology transformation for high-rate and long-life lithium-ion batteries. *RSC Adv.* **2017**, *7*, 21988–21996. [\[CrossRef\]](#)

136. Lo, W.-C.; Su, S.-H.; Chu, H.-J.; He, J.-L. TiO₂-CNTs grown on titanium as an anode layer for lithium-ion batteries. *Surf. Coat. Technol.* **2018**, *337*, 544–551. [\[CrossRef\]](#)
137. Zhang, X.; Cao, S.; Wu, Z.; Zhao, S.; Piao, L. Enhanced photocatalytic activity towards degradation and H₂ evolution over one dimensional TiO₂@MWCNTs heterojunction. *Appl. Surf. Sci.* **2017**, *402*, 360–368. [\[CrossRef\]](#)
138. Huang, S.-H.; Liao, S.-Y.; Wang, C.-C.; Kei, C.-C.; Gan, J.-Y.; Perng, T.-P. Direct formation of anatase TiO₂ nanoparticles on carbon nanotubes by atomic layer deposition and their photocatalytic properties. *Nanotechnology* **2016**, *27*, 405702. [\[CrossRef\]](#) [\[PubMed\]](#)
139. Kaushik, P.; Eliáš, M.; Michalička, J.; Hegemann, D.; Pytlíček, Z.; Nečas, D.; Zajíčková, L. Atomic layer deposition of titanium dioxide on multi-walled carbon nanotubes for ammonia gas sensing. *Surf. Coat. Technol.* **2019**, *370*, 235–243. [\[CrossRef\]](#)
140. Avasthi, P.; Balakrishnan, V. Tuning the Wettability of Vertically Aligned CNT–TiO₂ Hybrid Electrodes for Enhanced Supercapacitor Performance. *Adv. Mater. Interfaces* **2019**, *6*, 1801842. [\[CrossRef\]](#)
141. Moya, A.; Kemnade, N.; Osorio, M.R.; Cherevan, A.; Granados, D.; Eder, D.; Vilatela, J.J. Large area photoelectrodes based on hybrids of CNT fibres and ALD-grown TiO₂. *J. Mater. Chem. A* **2017**, *5*, 24695–24706. [\[CrossRef\]](#)
142. Li, M.; Zu, M.; Yu, J.; Cheng, H.; Li, Q.; Li, B. Controllable synthesis of core-sheath structured aligned carbon nanotube/titanium dioxide hybrid fibers by atomic layer deposition. *Carbon* **2017**, *123*, 151–157. [\[CrossRef\]](#)
143. Mombeshora, E.T.; Ndungu, P.G.; Jarvis, A.L.L.; Nyamori, V.O. The physical and electrochemical properties of nitrogen-doped carbon nanotube- and reduced graphene oxide-titania nanocomposites. *Mater. Chem. Phys.* **2018**, *213*, 102–112. [\[CrossRef\]](#)
144. El Marouazi, H.; Jiménez-Calvo, P.; Breniaux, E.; Colbeau-Justin, C.; Janowska, I.; Keller, V. Few Layer Graphene/TiO₂ Composites for Enhanced Solar-Driven H₂ Production from Methanol. *ACS Sust. Chem. Eng.* **2021**, *9*, 3633–3646. [\[CrossRef\]](#)
145. Siew, Q.Y.; Pang, E.L.; Loh, H.-S.; Tan, M.T.T. Highly sensitive and specific graphene/TiO₂ impedimetric immunosensor based on plant-derived tetravalent envelope glycoprotein domain III (EDIII) probe antigen for dengue diagnosis. *Biosens. Bioelectron.* **2021**, *176*, 112895. [\[CrossRef\]](#) [\[PubMed\]](#)
146. Liu, C.; Lin, Y.; Dong, Y.; Wu, Y.; Bao, Y.; Yan, H.; Ma, J. Fabrication and investigation on Ag nanowires/TiO₂ nanosheets/graphene hybrid nanocomposite and its water treatment performance. *Adv. Comp. Hybrid. Mater.* **2020**, *3*, 402–414. [\[CrossRef\]](#)
147. Otgonbayar, Z.; Cho, K.Y.; Oh, W.-C. Novel Micro and Nanostructure of a AgCuInS₂–Graphene–TiO₂ Ternary Composite for Photocatalytic CO₂ Reduction for Methanol Fuel. *ACS Omega* **2020**, *5*, 26389–26401. [\[CrossRef\]](#)
148. De Angelis, D.; Presel, F.; Jabeen, N.; Bignardi, L.; Lizzit, D.; Lacovig, P.; Lizzit, S.; Montini, T.; Fornasiero, P.; Alfè, D.; et al. Interfacial two-dimensional oxide enhances photocatalytic activity of graphene/titania via electronic structure modification. *Carbon* **2020**, *157*, 350–357. [\[CrossRef\]](#)
149. Falak, A.; Tian, Y.; Yan, L.; Zhang, X.; Xu, L.; Song, Z.; Dong, F.; Chen, P.; Zhao, M.; Wang, H.; et al. Simultaneous achievement of superior response and full recovery of titanium dioxide/graphene hybrid FET sensors for NH₃ through p- to n-mode switch. *Phys. Chem. Chem. Phys.* **2020**, *22*, 16701–16711. [\[CrossRef\]](#) [\[PubMed\]](#)
150. Fornasini, L.; Scaravonati, S.; Magnani, G.; Morengi, A.; Sidoli, M.; Bersani, D.; Bertoni, G.; Aversa, L.; Verucchi, R.; Riccò, M.; et al. In situ decoration of laser-scribed graphene with TiO₂ nanoparticles for scalable high-performance micro-supercapacitors. *Carbon* **2021**, *176*, 296–306. [\[CrossRef\]](#)
151. Cui, R.; Liu, S.; Guo, X.; Huang, H.; Wang, J.; Liu, B.; Li, Y.; Zhao, D.; Dong, J.; Sun, B. N-Doping Holey Graphene TiO₂–Pt Composite as Efficient Electrocatalyst for Methanol Oxidation. *ACS Appl. Energy Mater.* **2020**, *3*, 2665–2673. [\[CrossRef\]](#)
152. Long, B.; Zhang, J.; Luo, L.; Ouyang, G.; Balogun, M.-S.; Song, S.; Tong, Y. High pseudocapacitance boosts the performance of monolithic porous carbon cloth/closely packed TiO₂ nanodots as an anode of an all-flexible sodium-ion battery. *J. Mater. Chem. A* **2019**, *7*, 2626–2635. [\[CrossRef\]](#)
153. Kumar, K.Y.; Saini, H.; Pandiarajan, D.; Prashanth, M.K.; Parashuram, L.; Raghu, M.S. Controllable synthesis of TiO₂ chemically bonded graphene for photocatalytic hydrogen evolution and dye degradation. *Catal. Today* **2020**, *340*, 170–177. [\[CrossRef\]](#)
154. Wei, J.; Ping, H.; Xie, J.; Zou, Z.; Wang, K.; Xie, H.; Wang, W.; Lei, L.; Fu, Z. Bioprocess-Inspired Microscale Additive Manufacturing of Multilayered TiO₂/Polymer Composites with Enamel-Like Structures and High Mechanical Properties. *Adv. Funct. Mater.* **2020**, *30*, 1904880. [\[CrossRef\]](#)
155. El-Gendy, D.M.; Abdel Ghany, N.A.; Allam, N.K. Black titania nanotubes/spongy graphene nanocomposites for high-performance supercapacitors. *RSC Adv.* **2019**, *9*, 12555–12566. [\[CrossRef\]](#)
156. Rao, Z.; Lu, G.; Mahmood, A.; Shi, G.; Xie, X.; Sun, J. Deactivation and activation mechanism of TiO₂ and rGO/Er³⁺-TiO₂ during flowing gaseous VOCs photodegradation. *Appl. Catal. B Environ.* **2021**, *284*, 119813. [\[CrossRef\]](#)
157. Padmanabhan, N.T.; Jayaraj, M.K.; John, H. Graphene hybridized high energy faceted titanium dioxide for transparent self-cleaning coatings. *Catal. Today* **2020**, *348*, 63–71. [\[CrossRef\]](#)
158. Lu, Y.; Liu, Y.-X.; He, L.; Wang, L.-Y.; Liu, X.-L.; Liu, J.-W.; Li, Y.-Z.; Tian, G.; Zhao, H.; Yang, X.-H.; et al. Interfacial co-existence of oxygen and titanium vacancies in nanostructured TiO₂ for enhancement of carrier transport. *Nanoscale* **2020**, *12*, 8364–8370. [\[CrossRef\]](#)
159. Veera Manohara Reddy, Y.; Sravani, B.; Luczak, T.; Mallikarjuna, K.; Madhavi, G. An ultra-sensitive rifampicin electrochemical sensor based on titanium nanoparticles (TiO₂) anchored reduced graphene oxide modified glassy carbon electrode. *Coll. Surf. A* **2021**, *608*, 125533. [\[CrossRef\]](#)
160. Ye, F.; Wang, Z.; Mi, Y.; Kuang, J.; Jiang, X.; Huang, Z.; Luo, Y.; Shen, L.; Yuan, H.; Zhang, Z. Preparation of reduced graphene oxide/titanium dioxide composite materials and its application in the treatment of oily wastewater. *Coll. Surf. A* **2020**, *586*, 124251. [\[CrossRef\]](#)

161. Maarisetty, D.; Mahanta, S.; Sahoo, A.K.; Mohapatra, P.; Baral, S.S. Steering the Charge Kinetics in Dual-Functional Photocatalysis by Surface Dipole Moments and Band Edge Modulation: A Defect Study in TiO₂-ZnS-rGO Composites. *ACS Appl. Mater. Interfaces* **2020**, *12*, 11679–11692. [\[CrossRef\]](#)
162. Li, C.; Hu, R.; Lu, X.; Bashir, S.; Liu, J.L. Efficiency enhancement of photocatalytic degradation of tetracycline using reduced graphene oxide coordinated titania nanoplatelet. *Catal. Today* **2020**, *350*, 171–183. [\[CrossRef\]](#)
163. Carreño-Lizcano, M.I.; Gualdrón-Reyes, A.F.; Rodríguez-González, V.; Pedraza-Avella, J.A.; Niño-Gómez, M.E. Photoelectrocatalytic phenol oxidation employing nitrogen doped TiO₂-rGO films as photoanodes. *Catal. Today* **2020**, *341*, 96–103. [\[CrossRef\]](#)
164. Mokhtarifar, M.; Kaveh, R.; Bagherzadeh, M.; Lucotti, A.; Peddeferri, M.; Diamanti, M.V. Heterostructured TiO₂/SiO₂/γ-Fe₂O₃/rGO Coating with Highly Efficient Visible-Light-Induced Self-Cleaning Properties for Metallic Artifacts. *ACS Appl. Mater. Interfaces* **2020**, *12*, 29671–29683. [\[CrossRef\]](#) [\[PubMed\]](#)
165. Oladipo, H.; Garlisi, C.; Sa, J.; Lewin, E.; Al-Ali, K.; Palmisano, G. Unveiling the role of bisulfide in the photocatalytic splitting of H₂S in aqueous solutions. *Appl. Catal. B Environ.* **2020**, *270*, 118886. [\[CrossRef\]](#)
166. Hu, Y.; Wang, M.; Hu, F.; Wu, J.; Xu, L.; Xu, G.; Jian, Y.; Peng, X. Controllable construction of hierarchical TiO₂ supported on hollow rGO/P-HC heterostructure for highly efficient photocatalysis. *Coll. Surf. A* **2020**, *598*, 124831. [\[CrossRef\]](#)
167. Raja, A.; Rajasekaran, P.; Selvakumar, K.; Arivanandhan, M.; Asath Bahadur, S.; Swaminathan, M. Efficient Photoreduction of Hexavalent Chromium Using the Reduced Graphene Oxide-Sm₂MoO₆-TiO₂ Catalyst under Visible Light Illumination. *ACS Omega* **2020**, *5*, 6414–6422. [\[CrossRef\]](#) [\[PubMed\]](#)
168. Wu, Y.; Mu, H.; Cao, X.; He, X. Polymer-supported graphene-TiO₂ doped with nonmetallic elements with enhanced photocatalytic reaction under visible light. *J. Mater. Sci.* **2020**, *55*, 1577–1591. [\[CrossRef\]](#)
169. Zhao, W.; Ci, X. TiO₂ Nanoparticle/Fluorinated Reduced Graphene Oxide Nanosheet Composites for Lubrication and Wear Resistance. *ACS Appl. Nano Mater.* **2020**, *3*, 8732–8741. [\[CrossRef\]](#)
170. Zhang, H.; Zhao, Y.; Yang, X.; Zhao, G.; Zhang, D.; Huang, H.; Yang, S.; Wen, N.; Javid, M.; Fan, Z.; et al. A Facile Synthesis of Novel Amorphous TiO₂ Nanorods Decorated rGO Hybrid Composites with Wide Band Microwave Absorption. *Nanomaterials* **2020**, *10*, 2141. [\[CrossRef\]](#) [\[PubMed\]](#)
171. Gao, Y.; Yan, N.; Jiang, C.; Xu, C.; Yu, S.; Liang, P.; Zhang, X.; Liang, S.; Huang, X. Filtration-enhanced highly efficient photocatalytic degradation with a novel electrospun rGO@TiO₂ nanofibrous membrane: Implication for improving photocatalytic efficiency. *Appl. Catal. B Environ.* **2020**, *268*, 118737. [\[CrossRef\]](#)
172. Maiti, M.; Sarkar, M.; Liu, D. Mechanism of nicotine degradation and adsorption by a nano-TiO₂ engineered reduced graphene oxide composite in light variant conditions. *Catal. Sci. Technol.* **2020**, *10*, 2797–2809. [\[CrossRef\]](#)
173. Farooq, U.; Ahmed, F.; Pervez, S.A.; Rehman, S.; Pope, M.A.; Fichtner, M.; Roberts, E.P.L. A stable TiO₂-graphene nanocomposite anode with high rate capability for lithium-ion batteries. *RSC Adv.* **2020**, *10*, 29975–29982. [\[CrossRef\]](#)
174. Chen, M.; Wu, G.; Zhang, M.; Liu, J.; Zai, J.; Qian, X.; Yu, X. A highly efficient nano-graphite electron transport layer for high performance ZnO/Si solar cells. *Sustain. Energy Fuels* **2018**, *2*, 820–826. [\[CrossRef\]](#)
175. Yao, S.; Yuan, X.; Jiang, L.; Xiong, T.; Zhang, J. Recent Progress on Fullerene-Based Materials: Synthesis, Properties, Modifications, and Photocatalytic Applications. *Materials* **2020**, *13*, 2924. [\[CrossRef\]](#) [\[PubMed\]](#)
176. Gatti, T.; Menna, E.; Meneghetti, M.; Maggini, M.; Petrozza, A.; Lamberti, F. The Renaissance of fullerenes with perovskite solar cells. *Nano Energy* **2017**, *41*, 84–100. [\[CrossRef\]](#)
177. Regulska, E.; Rivera-Nazario, D.M.; Karpinska, J.; Plonska-Brzezinska, M.E.; Echegoyen, L. Zinc Porphyrin-Functionalized Fullerenes for the Sensitization of Titania as a Visible-Light Active Photocatalyst: River Waters and Wastewaters Remediation. *Molecules* **2019**, *24*, 1118. [\[CrossRef\]](#)
178. Amelot, D.; Ahmadpour, M.; Ros, Q.; Cruguel, H.; Casaretto, N.; Cossaro, A.; Floreano, L.; Madsen, M.; Witkowski, N. Deciphering Electron Interplay at the Fullerene/Sputtered TiO_x Interface: A Barrier-Free Electron Extraction for Organic Solar Cells. *ACS Appl. Mater. Interfaces* **2021**, *13*, 19460–19466. [\[CrossRef\]](#)
179. Mohapatra, D.; Nemala, S.S.; Sayed, M.S.; Shim, J.-J.; Mallick, S.; Bhargava, P.; Parida, S. Carbon nano-onion-powered optically transparent and economical dye-sensitized solar cells. *Nanoscale* **2020**, *12*, 20621–20630. [\[CrossRef\]](#) [\[PubMed\]](#)
180. Iglesias, D.; Atienzar, P.; Vázquez, E.; Herrero, M.A.; García, H. Carbon Nanohorns Modified with Conjugated Terthienyl/Terthiophene Structures: Additives to Enhance the Performance of Dye-Sensitized Solar Cells. *Nanomaterials* **2017**, *7*, 294. [\[CrossRef\]](#) [\[PubMed\]](#)
181. Lodermeier, F.; Costa, R.D.; Guldi, D.M. Implementation of Single-Walled Carbon Nanohorns into Solar Cell Schemes. *Adv. Energy Mater.* **2017**, *7*, 1601883. [\[CrossRef\]](#)
182. Iglesias, D.; Melle-Franco, M.; Kurbasic, M.; Melchionna, M.; Abrami, M.; Grassi, M.; Prato, M.; Marchesan, S. Oxidized nanocarbons-tripeptide supramolecular hydrogels: Shape matters! *ACS Nano* **2018**, *12*, 5530–5538. [\[CrossRef\]](#) [\[PubMed\]](#)
183. Kumar, S.; Nehra, M.; Kedia, D.; Dilbaghi, N.; Tankeshwar, K.; Kim, K.-H. Nanodiamonds: Emerging face of future nanotechnology. *Carbon* **2019**, *143*, 678–699. [\[CrossRef\]](#)
184. Melchionna, M.; Beltram, A.; Stopin, A.; Montini, T.; Lodge, R.W.; Khlobystov, A.N.; Bonifazi, D.; Prato, M.; Fornasiero, P. Magnetic shepherding of nanocatalysts through hierarchically-assembled Fe-filled CNTs hybrids. *Appl. Catal. B Environ.* **2018**, *227*, 356–365. [\[CrossRef\]](#)
185. Faraldos, M.; Bahamonde, A. Environmental applications of titania-graphene photocatalysts. *Catal. Today* **2017**, *285*, 13–28. [\[CrossRef\]](#)

186. Kusiak-Nejman, E.; Morawski, A.W. TiO₂/graphene-based nanocomposites for water treatment: A brief overview of charge carrier transfer, antimicrobial and photocatalytic performance. *Appl. Catal. B Environ.* **2019**, *253*, 179–186. [\[CrossRef\]](#)
187. Ampelli, C.; Tavella, F.; Perathoner, S.; Centi, G. Engineering of photoanodes based on ordered TiO₂-nanotube arrays in solar photo-electrocatalytic (PECa) cells. *Chem. Eng. J.* **2017**, *320*, 352–362. [\[CrossRef\]](#)
188. Al Jitan, S.; Palmisano, G.; Garlisi, C. Synthesis and Surface Modification of TiO₂-Based Photocatalysts for the Conversion of CO₂. *Catalysts* **2020**, *10*, 227. [\[CrossRef\]](#)
189. Kiss, J.; Sápi, A.; Tóth, M.; Kukovecz, Á.; Kónya, Z. Rh-induced Support Transformation and Rh Incorporation in Titanate Structures and Their Influence on Catalytic Activity. *Catalysts* **2020**, *10*, 212. [\[CrossRef\]](#)
190. Wada, K.; Yu, H.; Feng, Q. Titania-supported iridium catalysts for dehydrogenative synthesis of benzimidazoles. *Chin. Chem. Lett.* **2020**, *31*, 605–608. [\[CrossRef\]](#)
191. Yu, Z.; Liu, H.; Zhu, M.; Li, Y.; Li, W. Interfacial Charge Transport in 1D TiO₂ Based Photoelectrodes for Photoelectrochemical Water Splitting. *Small* **2021**, *17*, 1903378. [\[CrossRef\]](#) [\[PubMed\]](#)
192. Li, B.; Wu, S.; Gao, X. Theoretical calculation of a TiO₂-based photocatalyst in the field of water splitting: A review. *Nanotechnol. Rev.* **2020**, *9*, 1080–1103. [\[CrossRef\]](#)
193. Tada, H.; Naya, S.-I. Atomic Level Interface Control of SnO₂-TiO₂ Nanohybrids for the Photocatalytic Activity Enhancement. *Catalysts* **2021**, *11*, 205. [\[CrossRef\]](#)
194. Syed, M.H.; Tabassum, H.; Moeen, F.; Qasim, A.; Shafaqat, A.; Muhammad, R.; Abdullah, I.H.; Madhumita, B.R.; Shahzad, A.S.C. Emerging Aspects of Photo-catalysts (TiO₂ & ZnO) Doped Zeolites and Advanced Oxidation Processes for Degradation of Azo Dyes: A Review. *Curr. Anal. Chem.* **2021**, *17*, 82–97.
195. de Brito, J.F.; Tavella, F.; Genovese, C.; Ampelli, C.; Zanon, M.V.B.; Centi, G.; Perathoner, S. Role of CuO in the modification of the photocatalytic water splitting behavior of TiO₂ nanotube thin films. *Appl. Catal. B Environ.* **2018**, *224*, 136–145. [\[CrossRef\]](#)
196. Abed, J.; Rajput, N.S.; Moutaouakil, A.E.; Jouiad, M. Recent Advances in the Design of Plasmonic Au/TiO₂ Nanostructures for Enhanced Photocatalytic Water Splitting. *Nanomaterials* **2020**, *10*, 2260. [\[CrossRef\]](#) [\[PubMed\]](#)
197. Ampelli, C.; Tavella, F.; Genovese, C.; Perathoner, S.; Favaro, M.; Centi, G. Analysis of the factors controlling performances of Au-modified TiO₂ nanotube array based photoanode in photo-electrocatalytic (PECa) cells. *J. Energy Chem.* **2017**, *26*, 284–294. [\[CrossRef\]](#)
198. Abdelnasser, S.; Al Sakka, R.; Palmisano, G. Environmental and energy applications of TiO₂ photoanodes modified with alkali metals and polymers. *J. Environ. Chem. Eng.* **2021**, *9*, 104873. [\[CrossRef\]](#)
199. Hua, L.; Yin, Z.; Cao, S. Recent Advances in Synthesis and Applications of Carbon-Doped TiO₂ Nanomaterials. *Catalysts* **2020**, *10*, 1431. [\[CrossRef\]](#)
200. Kiwi, J.; Rtimi, S. Insight into the interaction of magnetic photocatalysts with the incoming light accelerating bacterial inactivation and environmental cleaning. *Appl. Catal. B Environ.* **2021**, *281*, 119420. [\[CrossRef\]](#)
201. Arulmozhi, S.; Ezhil Arasi, S. Size controlled synthesis of gadolinium doped titanium dioxide nanoparticles by low temperature hydrothermal method towards effective photovoltaic application. *Mater. Today Proc.* **2020**, *8*, 456.
202. Li, J.; Chu, B.; Xie, Z.; Deng, Y.; Zhou, Y.; Dong, L.; Li, B.; Chen, Z. Mechanism and DFT Study of Degradation of Organic Pollutants on Rare Earth Ions Doped TiO₂ Photocatalysts Prepared by Sol-Hydrothermal Synthesis. *Catal. Lett.* **2021**. [\[CrossRef\]](#)
203. Perini, J.A.L.; Tavella, F.; Ferreira Neto, E.P.; Zanon, M.V.B.; Ribeiro, S.J.L.; Giusi, D.; Centi, G.; Perathoner, S.; Ampelli, C. Role of nanostructure in the behaviour of BiVO₄-TiO₂ nanotube photoanodes for solar water splitting in relation to operational conditions. *Sol. Energy Mater. Sol. Cells* **2021**, *223*, 110980. [\[CrossRef\]](#)
204. Ren, Y.; Han, Q.; Su, Q.; Yang, J.; Zhao, Y.; Wen, H.; Jiang, Z. Effects of 4d transition metals doping on the photocatalytic activities of anatase TiO₂ (101) surface. *Int. J. Quantum Chem.* **2021**, *121*, e26683. [\[CrossRef\]](#)
205. Cheng, C.; Fang, W.-H.; Long, R.; Prezhdo, O.V. Water Splitting with a Single-Atom Cu/TiO₂ Photocatalyst: Atomistic Origin of High Efficiency and Proposed Enhancement by Spin Selection. *J. Am. Chem. Soc.* **2021**, *143*, 550–559.
206. Bhol, P.; Yadav, S.; Altaee, A.; Saxena, M.; Misra, P.K.; Samal, A.K. Graphene-Based Membranes for Water and Wastewater Treatment: A Review. *ACS Appl. Nano Mater.* **2021**, *4*, 3274–3293. [\[CrossRef\]](#)
207. Som, I.; Roy, M.; Saha, R. Advances in Nanomaterial-based Water Treatment Approaches for Photocatalytic Degradation of Water Pollutants. *ChemCatChem* **2020**, *12*, 3409–3433. [\[CrossRef\]](#)
208. Mancuso, A.; Sacco, O.; Vaiano, V.; Sannino, D.; Pragliola, S.; Venditto, V.; Morante, N. Visible light active Fe-Pr co-doped TiO₂ for water pollutants degradation. *Catal. Today* **2021**. [\[CrossRef\]](#)
209. Rashid, R.; Shafiq, I.; Iqbal, M.J.; Shabir, M.; Akhter, P.; Hamayun, M.H.; Ahmed, A.; Hussain, M. Synergistic effect of NS co-doped TiO₂ adsorbent for removal of cationic dyes. *J. Environ. Chem. Eng.* **2021**, *9*, 105480. [\[CrossRef\]](#)
210. Zhang, L.; Moralejo, C.; Anderson, W.A. A review of the influence of humidity on photocatalytic decomposition of gaseous pollutants on TiO₂-based catalysts. *Can. J. Chem. Eng.* **2020**, *98*, 263–273. [\[CrossRef\]](#)
211. Hu, X.; Hu, X.; Peng, Q.; Zhou, L.; Tan, X.; Jiang, L.; Tang, C.; Wang, H.; Liu, S.; Wang, Y.; et al. Mechanisms underlying the photocatalytic degradation pathway of ciprofloxacin with heterogeneous TiO₂. *Chem. Eng. J.* **2020**, *380*, 122366. [\[CrossRef\]](#)
212. Hadei, M.; Mesdaghinia, A.; Nabizadeh, R.; Mahvi, A.H.; Rabbani, S.; Naddafi, K. A comprehensive systematic review of photocatalytic degradation of pesticides using nano TiO₂. *Environ. Sci. Pollut. Res.* **2021**, *28*, 13055–13071. [\[CrossRef\]](#)
213. Zhang, S.; He, Z.; Li, X.; Zhang, J.; Zang, Q.; Wang, S. Building heterogeneous nanostructures for photocatalytic ammonia decomposition. *Nanoscale Adv.* **2020**, *2*, 3610–3623. [\[CrossRef\]](#)

214. Vikrant, K.; Kim, K.-H.; Dong, F.; Giannakoudakis, D.A. Photocatalytic Platforms for Removal of Ammonia from Gaseous and Aqueous Matrixes: Status and Challenges. *ACS Catal.* **2020**, *10*, 8683–8716. [\[CrossRef\]](#)
215. Meng, A.; Zhang, L.; Cheng, B.; Yu, J. Dual Cocatalysts in TiO₂ Photocatalysis. *Adv. Mater.* **2019**, *31*, 1807660. [\[CrossRef\]](#)
216. Gul, I.; Sayed, M.; Shah, N.S.; Rehman, F.; Khan, J.A.; Gul, S.; Bibi, N.; Iqbal, J. A novel route for catalytic activation of peroxymonosulfate by oxygen vacancies improved bismuth-doped titania for the removal of recalcitrant organic contaminant. *Environ. Sci. Pollut. Res.* **2021**, *28*, 23368–23385. [\[CrossRef\]](#)
217. Raut, S.S.; Kamble, S.P.; Kulkarni, P.S. Improved photocatalytic efficiency of TiO₂ by doping with tungsten and synthesizing in ionic liquid: Precise kinetics-mechanism and effect of oxidizing agents. *Environ. Sci. Pollut. Res.* **2021**, *28*, 17532–17545. [\[CrossRef\]](#) [\[PubMed\]](#)
218. Saito, K.; Orikasa, S.; Asakura, Y.; Ide, Y.; Sugahara, Y.; Ogasawara, M.; Yin, S.; Kato, S. Ni-Doped Protonated Layered Titanate/TiO₂ Composite with Efficient Photocatalytic Activity for NO_x Decomposition Reactions. *Int. J. Photoen.* **2021**, *2021*, 8847956. [\[CrossRef\]](#)
219. Ziental, D.; Czarczynska-Goslinska, B.; Mlynarczyk, D.T.; Glowacka-Sobotta, A.; Stanisz, B.; Goslinski, T.; Sobotta, L. Titanium Dioxide Nanoparticles: Prospects and Applications in Medicine. *Nanomaterials* **2020**, *10*, 387. [\[CrossRef\]](#) [\[PubMed\]](#)
220. Sharma, R.; Jafari, S.M.; Sharma, S. Antimicrobial bio-nanocomposites and their potential applications in food packaging. *Food Control.* **2020**, *112*, 107086. [\[CrossRef\]](#)
221. Liao, C.; Li, Y.; Tjong, S.C. Visible-Light Active Titanium Dioxide Nanomaterials with Bactericidal Properties. *Nanomaterials* **2020**, *10*, 124. [\[CrossRef\]](#)
222. Raluca, I.; Madalina Georgiana, N.; Anca, M.; Valentina, M.; Patricia, N.; Patrik, S.; Anisoara, C. Drug Delivery Systems Based on Titania Nanotubes and Active Agents for Enhanced Osseointegration of Bone Implants. *Curr. Med. Chem.* **2020**, *27*, 854–902.
223. Chopra, D.; Gulati, K.; Ivanovski, S. Understanding and optimizing the antibacterial functions of anodized nano-engineered titanium implants. *Acta Biomater.* **2021**, *127*, 80–101. [\[CrossRef\]](#)
224. Masikini, M.; Chowdhury, M.; Nemraoui, O. Review—Metal Oxides: Application in Exhaled Breath Acetone Chemiresistive Sensors. *J. Electrochem. Soc.* **2020**, *167*, 037537. [\[CrossRef\]](#)
225. Meesombad, K.; Sato, N.; Pitiphattharabun, S.; Panomsuwan, G.; Techapiesancharoenkij, R.; Surawathanawises, K.; Wongchoosuk, C.; Boonsalee, S.; Pee, J.H.; Jongprateep, O. Zn-doped TiO₂ nanoparticles for glutamate sensors. *Ceram. Int.* **2021**. [\[CrossRef\]](#)
226. Li, J.; Wang, X.; Duan, H.; Wang, Y.; Luo, C. Ultra-sensitive determination of epinephrine based on TiO₂-Au nanoclusters supported on reduced graphene oxide and carbon nanotube hybrid nanocomposites. *Mater. Sci. Eng. C* **2016**, *64*, 391–398. [\[CrossRef\]](#) [\[PubMed\]](#)
227. Li, G.; Wu, J.; Jin, H.; Xia, Y.; Liu, J.; He, Q.; Chen, D. Titania/Electro-Reduced Graphene Oxide Nanohybrid as an Efficient Electrochemical Sensor for the Determination of Allura Red. *Nanomaterials* **2020**, *10*, 307. [\[CrossRef\]](#) [\[PubMed\]](#)
228. Murali, G.; Reddeppa, M.; Reddy, C.S.; Park, S.; Chandrakalavathi, T.; Kim, M.-D.; In, I. Enhancing the Charge Carrier Separation and Transport via Nitrogen-Doped Graphene Quantum Dot-TiO₂ Nanoplate Hybrid Structure for an Efficient NO Gas Sensor. *ACS Appl. Mater. Interfaces* **2020**, *12*, 13428–13436. [\[CrossRef\]](#)
229. Vital-Grappin, A.D.; Ariza-Tarazona, M.C.; Luna-Hernández, V.M.; Villarreal-Chiu, J.F.; Hernández-López, J.M.; Siligardi, C.; Cedillo-González, E.I. The Role of the Reactive Species Involved in the Photocatalytic Degradation of HDPE Microplastics Using C,N-TiO₂ Powders. *Polymers* **2021**, *13*, 999. [\[CrossRef\]](#)
230. Valenti, G.; Boni, A.; Melchionna, M.; Cargnello, M.; Nasi, L.; Bertoni, G.; Gorte, R.J.; Marcaccio, M.; Rapino, S.; Bonchio, M.; et al. Co-axial heterostructures integrating palladium/titanium dioxide with carbon nanotubes for efficient electrocatalytic hydrogen evolution. *Nat. Commun.* **2016**, *7*, 13549. [\[CrossRef\]](#)
231. Rajaraman, T.S.; Parikh, S.P.; Gandhi, V.G. Black TiO₂: A review of its properties and conflicting trends. *Chem. Eng. J.* **2020**, *389*, 123918. [\[CrossRef\]](#)
232. Sun, K.; Fang, Y.; Chi, L. On-Surface Synthesis on Nonmetallic Substrates. *ACS Mater. Lett.* **2021**, *3*, 56–63. [\[CrossRef\]](#)
233. Li, Q.; Anpo, M.; Wang, X. Application of photoluminescence spectroscopy to elucidate photocatalytic reactions at the molecular level. *Res. Chem. Intermed.* **2020**, *46*, 4325–4344. [\[CrossRef\]](#)
234. Fan, J.; Kotov, N.A. Chiral Nanoceramics. *Adv. Mater.* **2020**, *32*, 1906738. [\[CrossRef\]](#) [\[PubMed\]](#)
235. Wang, C.; Liu, S.; Duan, Y.; Huang, Z.; Che, S. Hard-templating of chiral TiO₂ nanofibres with electron transition-based optical activity. *Sci. Technol. Adv. Mater.* **2015**, *16*, 054206. [\[CrossRef\]](#) [\[PubMed\]](#)
236. Shopsowitz, K.E.; Stahl, A.; Hamad, W.Y.; MacLachlan, M.J. Hard Templating of Nanocrystalline Titanium Dioxide with Chiral Nematic Ordering. *Angew. Chem. Int. Ed.* **2012**, *51*, 6886–6890. [\[CrossRef\]](#) [\[PubMed\]](#)
237. Bondavalli, P.; Martin, M.B.; Hamidouche, L.; Montanaro, A.; Trompeta, A.-F.; Charitidis, C.A. Nano-Graphitic based Non-Volatile Memories Fabricated by the Dynamic Spray-Gun Deposition Method. *Micromachines* **2019**, *10*, 95. [\[CrossRef\]](#) [\[PubMed\]](#)
238. Ishaq, S.; Kanwal, F.; Atiq, S.; Moussa, M.; Azhar, U.; Losic, D. Dielectric Properties of Graphene/Titania/Polyvinylidene Fluoride (G/TiO₂/PVDF) Nanocomposites. *Materials* **2020**, *13*, 205. [\[CrossRef\]](#)
239. Huang, K.; Wang, T.; Jin, M.; Wu, L.; Wang, J.F.; Li, S.; Qi, D.-C.; Cheng, S.; Li, Y.; Chen, J.; et al. Bipolar Conduction and Giant Positive Magnetoresistance in Doped Metallic Titanium Oxide Heterostructures. *Adv. Mater. Interfaces* **2021**, *8*, 2002147. [\[CrossRef\]](#)
240. Wu, T.-S.; Syu, L.-Y.; Lin, B.-H.; Weng, S.-C.; Jeng, H.-T.; Huang, Y.-S.; Soo, Y.-L. Reduction of dopant ions and enhancement of magnetic properties by UV irradiation in Ce-doped TiO₂. *Sci. Rep.* **2021**, *11*, 7668. [\[CrossRef\]](#)